

Showcasing research from Professor Ryuji Yokokawa's laboratory, Department of Micro Engineering, Kyoto University, Japan.

Vascular microphysiological systems (MPS): biologically relevant and potent models

Vascular microphysiological systems (MPSs) are gaining increasing significance due to advancements in microvascular patterning, three-dimensional organization, and both cellular and acellular modelling. These improvements have enhanced their biological fidelity, making vascular MPS powerful tools for investigating vascular biology in relation to key physical parameters such as flow, stretch, and permeability. In parallel, their translational relevance continues to grow, with promising applications in disease and cancer modelling, immunological studies, and preclinical drug screening. Together, these features position vascular MPS as versatile platforms bridging basic science and biomedical innovation.

### As featured in:



See Ryuji Yokokawa *et al.*,  
*Lab Chip*, 2025, **25**, 4221.



Cite this: *Lab Chip*, 2025, **25**, 4221

## Vascular microphysiological systems (MPS): biologically relevant and potent models

Lucas Breuil, <sup>a</sup> Atsuya Kitada, <sup>a</sup> Sachin Yadav, <sup>a</sup> Hang Zhou, <sup>abc</sup> Kazuya Fujimoto <sup>a</sup> and Ryuji Yokokawa <sup>\*a</sup>

Extensive research has focused on the vasculature, aiming to understand its structural characteristics, functions, interactions with surrounding tissues, and the mechanisms underlying vascular-related pathologies. However, advancing our understanding of vascular biology requires more complex and physiologically relevant models that integrate physical, chemical, and biological factors. Traditional *in vitro* dish models cannot replicate three-dimensional (3D) architecture, multi-cell-type interactions, and extracellular environments. *In vivo* animal models, while more complex, present ethical concerns, high costs, and limited relevance to human physiology. As a result, increasing attention is being directed toward *in vitro* models, specifically vascular microphysiological systems (MPS) based on organ-on-a-chip (OoC) technologies. This review highlights the relevance and potency of vascular MPS, which leverage microfluidic channels and 3D structures to mimic the physiological environment, incorporate diverse cellular and acellular components, and support complex biological processes. Vascular MPS are already enabling deep investigation into vascular responses to physiological cues, interactions with healthy and pathological tissues, and applications in disease modeling and drug development.

Received 6th January 2025,  
Accepted 6th June 2025

DOI: 10.1039/d5lc00014a

rsc.li/loc

### I. Introduction

Vasculature is one of the most critical systems for maintaining homeostasis, enabling blood circulation, delivering oxygen and nutrients to all organs, and removing waste for excretion. Given its essential role, dysregulation of the vasculature is related to numerous diseases and pathologies. Two major pathologies directly affecting vasculature are cardiovascular diseases, representing 37% of noncommunicable disease-related deaths in 2021, with roughly 20 million deaths globally,<sup>1</sup> and hypertension, affecting roughly 1.28 billion people worldwide.<sup>2</sup> In addition, non-vascular-specific diseases, such as various degenerative diseases<sup>3</sup> and diabetes,<sup>4</sup> either result from or contribute to vascular dysfunction. Tumor vasculature also plays a key role in cancer progression and is recognized as one of the hallmarks of cancer.<sup>5,6</sup>

Traditional research models, including cell culture, animal models, and human studies, provided significant insights into vascular biology. However, each model has inherent limitations, including organizational relevance,<sup>7,8</sup> proximity to human

physiology,<sup>9,10</sup> sample availability,<sup>11</sup> or ethical concerns.<sup>10,11</sup> Dish-based cell culture lacks physiological complexity, often relying on limited cell lines, facing challenges with multi-cell type co-culture and lacking 3D environment recapitulation. Animal models, while offering *in vivo* complexity, differ significantly from human physiology and raise both ethical and cost-related concerns. Human tissue studies, despite their physiological relevance and complexity, are constrained by limited availability, high sample to sample variability, ethical considerations, and lower experimental control.

In contrast, microphysiological systems (MPS) offer a promising alternative. These *in vitro* models incorporate diverse physiologically relevant cellular and acellular components, recapitulate 3D tissue architecture, and allow controlled manipulation of physical and chemical parameters. MPS are generally cost-effective, relatively user-friendly, and raise fewer ethical questions compared to traditional models. In recent years, the definition of MPS has come to encompass a broad range of technologies, including 3D cultures, 3D bioprinting, organoids, and organ-on-a-chip (OoC). Among these, MPS based on OoC technologies offer distinct advantages for vascular studies due to their microfluidic properties. Accordingly, this review uses the term “MPS” specifically to refer to OoC-based technologies, with other systems mentioned explicitly when relevant.

In this review, we highlight the current and recent advances in the use of MPS to model the vasculature, emphasizing their

<sup>a</sup> Department of Micro Engineering, Kyoto University, Kyoto Daigaku-katsura, Nishikyo-ku, Kyoto 615-8540, Japan. E-mail: yokokawa.yuji.8c@kyoto-u.ac.jp

<sup>b</sup> Human Organ Physiopathology Emulation System, Institute of Zoology, Chinese Academy of Sciences, Beijing 100101, China

<sup>c</sup> Beijing Institute for Stem Cell and Regenerative Medicine, Beijing 100101, China

growing biological relevance. We first briefly introduce the vascular anatomy to underscore the complexity of *in vivo* vasculature and the need for appropriate models. This is followed by a description of the fabrication processes of polydimethylsiloxane (PDMS)-based MPS, particularly focusing on soft lithography. We then discuss how design strategies, both pre-patterning and self-organizing, enhance architectural fidelity. The physiological relevance of vascular MPS is further explored through considerations of cellular and acellular components. Finally, we highlight the power of vascular MPS in advancing our understanding of vascular mechanobiology, physiology, and pathophysiology.

### I.1) Anatomy of the vascular system

The vascular system consists of blood vessels, looping from the heart to the different organs and back to the heart, and exhibits hierarchical organization, from arteries and arterioles to capillaries, then to venules and veins.

Arteries, arterioles, venules, and veins share a common structural organization, consisting of three distinct layers<sup>12</sup> (Fig. 1A). The innermost layer, tunica intima, comprises a continuous monolayer of endothelial cells (ECs) supported by a thin basement membrane. The middle layer is the tunica media, which is primarily composed of smooth muscle cells (SMCs) and has a vessel-type-dependent thickness. The outermost layer, the tunica externa, consists of fibroblasts embedded within an extracellular matrix (ECM).

Regarding the tunica media, arteries and arterioles are characterized by a thick layer, making them more contractile and elastic. SMCs in this layer regulate vessel stiffness through interaction with the ECM and are responsible for vascular contraction and dilation.<sup>13</sup> In contrast, venules and veins have a thinner tunica media with limited contractile ability, relying instead on the contraction of surrounding muscles to facilitate blood flow.<sup>14</sup> In the tunica externa, fibroblasts maintain the structural integrity and elasticity of the vascular wall by secreting ECM components, providing structural support, and anchoring the vessel to surrounding tissues.<sup>15</sup> Despite this shared structural organization, vessel diameter and morphology vary widely. Arteries are generally round in cross-section, with elastic arteries ranging from 10 mm in diameter to 25 mm for the aorta, while muscular arteries range from 1 to 10 mm<sup>16</sup> (Fig. 1A). Arterioles typically have diameters below 400  $\mu\text{m}$ . Veins are more ovoid in shape, with diameters ranging between 5 mm and 15 mm, to 30 mm in the case of the vena cava<sup>16</sup> (Fig. 1A).

Capillaries are composed solely of a monolayer of microvascular ECs, which can either be continuous, fenestrated, or discontinuous, depending on their function and anatomical location in the body.<sup>12</sup> Capillaries have diameters typically below 10  $\mu\text{m}$ ,<sup>16,17</sup> but form a dense vascular bed in direct contact with tissues. Their thin walls and extensive surface area make them the primary site of oxygen, nutrient, and waste exchange.<sup>17</sup> The direct surrounding of capillaries is composed of pericytes lining the

vessels (Fig. 1A), which regulate the formation and maintenance of capillary networks, as well as blood flow.<sup>17</sup>

It is important to highlight the presence of specialized vascular structures within the vascular system, with the examples of the aortic arch and venous valves. The aortic arch is located in the initial segment of the aortic artery, between the ascending and descending aorta, and gives rise to three major arteries supplying the upper body.<sup>18</sup> The aorta branch's primary functions are to redistribute blood flow between the aorta and the three arterial branches and to help regulate blood pressure through mechanosensory feedback mechanisms.<sup>18</sup> In contrast, venous valves are a morphological feature specific to veins in the lower extremities. These valves consist of two leaflets (bicuspid valves) formed by protrusions of the tunica intima, reinforced by collagen and elastic fibers, and lined with endothelial cells.<sup>19</sup> The main role is to prevent the backflow of blood back to the lower body, counteracting the effects of gravity and the lack of continuous muscular peristalsis.<sup>19</sup>

### I.2) Vascular MPS fabrication methods

MPS can be fabricated using a variety of techniques. In recent years, 3D printing techniques using plastics or biopolymers have gained prominence and have been extensively reviewed.<sup>20–25</sup> Some techniques are based on the direct printing of devices using UV light to cure a photosensitive polymer, such as stereolithography (SLA), digital light processing (DLP), or two-photon photopolymerization (TPP). Other direct-printing techniques rely on the extrusion and deposition of resins or gels, such as fused UV-direct ink writing (UV-DIW), fused deposition modeling (FDM), coaxial extrusion, and material jetting (MJ). Additionally, indirect 3D-printing is commonly used for 3D-printed molds and sacrificial templates.<sup>24</sup>

Various types of polymers can be used in these fabrication methods. Plastic polymers, notably including PDMS, polystyrene (PS), polyethylene terephthalate (PET), and poly(methyl methacrylate) (PMMA), are favored for their ability to form rigid structures with relatively good resolution, transparency, and biocompatibility. Resins, like polyethylene glycol monomethacrylate (PEGMA), are also employed, despite limitations such as opacity and poor biocompatibility. Bioprinting, which uses naturally derived materials such as alginate, collagen, gelatin, or ECM, has become increasingly widespread in recent years.<sup>23</sup>

This review, however, focuses primarily on PDMS-based devices fabricated using soft lithography, as it remains the most common method used for MPS fabrication, since the original lung-on-chip.<sup>26</sup> The soft lithography process begins with the design of a photomask using computer-aided design (CAD) software.<sup>27</sup> Then, UV light is projected through the photomask onto a silicon wafer coated with a thin layer of photosensitive resin. Depending on the type of photoresist used, the resin is either crosslinked (negative resist) or dissolved (positive resist) upon exposure to UV light. The

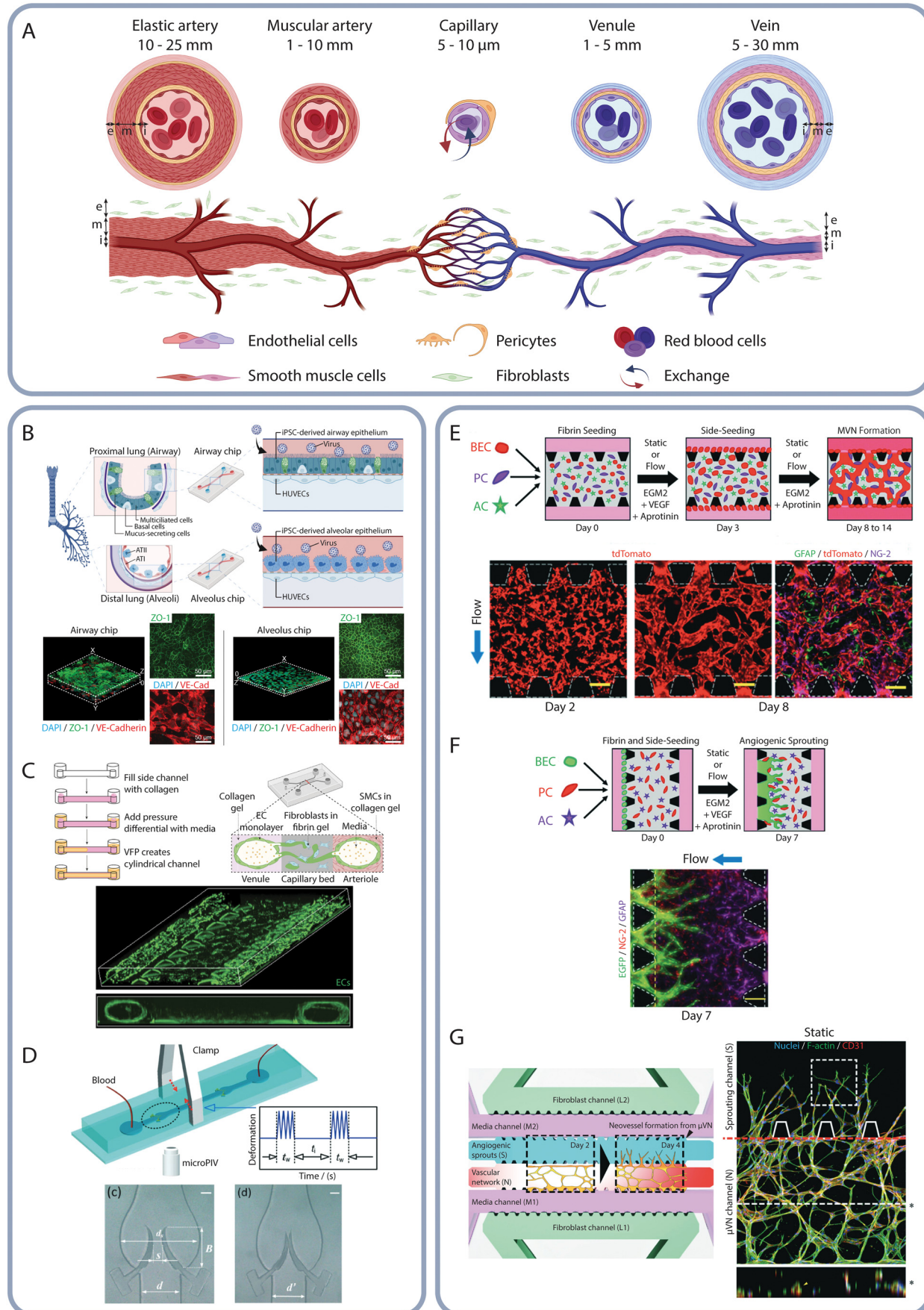


**Fig. 1** Blood vessel architecture and diversity of vascular MPS models. A) The vascular system is composed of different-order vessels: arteries, arterioles, capillaries, venules, and veins. Vessels have specific structures and components, giving them diverse properties such as elasticity, permeability, and functions. Red blood cells flow through the vasculature. Gas, nutrient, and waste exchanges occur at the capillary-tissue interfaces. Tunica intima (i), tunica media (m), and tunica externa (e) are shown. Created in BioRender. Fujimoto, K. (2025) <https://BioRender.com/l33p826>. B-D) Pre-patterning methods to obtain vascular MPS. B) 2D bilayer devices modeling lung-on-chip.<sup>29</sup> The tissue channel is composed of either airways or alveolar epithelium, while the vascular channel is lined with ECs. SARS-CoV-2 infection has been recapitulated using these devices. Scale bars: 50  $\mu$ m. C) Using a viscous finger patterning method, 3D pre-patterned channels have been obtained and lined with ECs.<sup>35</sup> The figure has been rearranged from the original. D) A venous valve design, with two valves and a clamp in between, which mimics muscle contraction.<sup>42</sup> (c) and (d) The open and closed state, respectively.  $t_i$  is the interval period with no clamping.  $t_w$  is the working period with ongoing clamping.  $d_s$ ,  $S$ ,  $d$ ,  $d'$ , and  $B$  are various size parameters of the device. Scale bars: 100  $\mu$ m. E-G) Self-organizing methods are used to obtain 3D vascular networks *on-chip*, relying on either vasculogenesis or angiogenesis processes. E) A vasculogenesis-based method using a 3-channel device with micropillars.<sup>53</sup> Gel, containing a mixture of ECs, pericytes, and astrocytes, is injected into the central channel, and the vascular network forms spontaneously in 8 days. Scale bars: 200  $\mu$ m. The figure has been rearranged from the original. F) An angiogenesis-based method using the same device as E).<sup>53</sup> Gel, containing only pericytes and astrocytes, is injected into the central channel. ECs are seeded on the side of the gel and sprout over the course of 7 days. Scale bar: 200  $\mu$ m. The figure has been rearranged from the original. G) 6-channel device encapsulating both vasculogenesis and angiogenesis processes.<sup>57</sup> The vascular network forms during the first 2 days and sprouts start thereafter for 3 days. The figure has been rearranged from the original. All figures have been edited to enhance readability.

resulting master mold is often treated *via* siloxane-based coating to facilitate demolding. Liquid PDMS is then poured onto the master mold, degassed to remove air bubbles, and thermally cured. Finally, PDMS layers are cut, punctured, treated, and bonded to form the desired device structure.

Compared to other fabrication techniques, soft lithography enables high-resolution patterning. Qin *et al.* described the different resolutions in each step of soft lithography using a commercial printer.<sup>27</sup> Mask design can reach down to 1  $\mu$ m resolution, photomask printing down to 20  $\mu$ m, master fabrication down to 1  $\mu$ m, and PDMS stamping down to 500 nm. Even higher resolution can be achieved using chromium (Cr) photomasks with conventional photolithography. Nevertheless, typical soft lithography workflows can routinely produce devices with an approximate resolution of 20  $\mu$ m. Beyond resolution, PDMS offers several other advantages that make it a widespread material for MPS fabrication, including low cost, optical transparency, gas permeability, and biocompatibility.<sup>28</sup> However, notable drawbacks of PDMS include its inherent hydrophobicity and the tendency to absorb small molecules.<sup>28</sup> Owing to many favorable characteristics, PDMS has been extensively used in the field and remains the predominant material for MPS fabrication. This widespread adoption justifies the focus of the present review on PDMS-based systems.

## II. Vascular MPS as highly relevant models

### II.1) Design considerations for architectural relevance

Vascular MPS can be constructed using two methods: pre-patterning or self-organizing methods. While pre-patterning methods focus on either endothelium-tissue interfaces or blood vessel structure modeling, self-organizing methods aim to reproduce physiological phenomena *on-chip*.

**Pre-patterning methods: 2D and 3D.** In pre-patterning methods, cells adhere to the walls of pre-existing vessel structures, relying on microfabricated channel designs to define vessel diameter, length, connecting points, or overall

shape. The most traditional and widely used model, derived from Huh *et al.*'s original lung-on-chip,<sup>26</sup> is the two-dimensional (2D) bilayer structure. The designs consist of two superimposed channels separated by a porous membrane. A vascular side is lined with ECs and exposed to either static<sup>29,30</sup> or flow<sup>31,32</sup> conditions, while an organ side contains organ-specific cells, which can be epithelial cells,<sup>29,30</sup> or perivascular cells<sup>31,32</sup> (Fig. 1B). Variations in these 2D designs arise from differences in channel dimensions (e.g., length, width, height) and contact areas. These 2D vascular MPS are commonly used to study interactions between vasculature and tissues, offering valuable insights into both healthy<sup>26,32</sup> and pathological<sup>29–31</sup> conditions. However, although 2D bilayer models allow the application of physical cues such as flow or stretch, they share several limitations with culture on insets: namely, being restricted to bilayer co-culture and lacking 3D environments and structural complexity.

For this reason, pre-patterned 3D designs have recently gained momentum for their improved physiological relevance. However, constructing 3D pre-patterned models presents greater challenges, as traditional soft lithography techniques produce rectangular microfluidic channels that deviate from the circular geometry of *in vivo* blood vessels. While some studies turn to alternative fabrication methods such as 3D printing<sup>33</sup> and bioprinting,<sup>21</sup> some have succeeded in obtaining 3D vessels even within rectangular channels using viscous finger patterning.<sup>34–36</sup> This technique involves injecting gel into the channel and applying pressure or aspiration at one of the ends. Thus, removing the gel from the channel and leaving behind a tubular structure resembling the circular geometry of *in vivo* blood vessels. Chen *et al.* demonstrated the effectiveness of viscous finger patterning by creating a hierarchical microvasculature-on-chip that incorporated an arteriole surrounded by SMCs, capillaries, and a venule within a single device<sup>35</sup> (Fig. 1C). Simpler methods consist of seeding ECs on two or all walls to obtain lumen formation.<sup>37,38</sup> Overall, these 3D models improve vessel architecture modeling, both in shape and

organization, with the integration of perivascular cells such as SMCs<sup>35</sup> or macrophages.<sup>36</sup>

Pre-patterned devices have also been utilized to model specific vascular structures, such as the aortic branch and venous valves. For instance, Li *et al.* developed a device with an arched channel and three branches connected to the peak of the arch.<sup>39</sup> This model was used to assess shear stress distribution within the device and thrombosis conditions. In the case of venous valves, several studies have proposed variations of valve designs to investigate thrombosis.<sup>39-44</sup> While most studies employed fixed valve structures, one specific study introduced small, flexible leaflets made of polyethylene glycol diacrylate (PEG-DA) that respond to flow direction, opening under forward flow and closing under backflow, thereby mimicking native valve behavior<sup>42</sup> (Fig. 1D). Additionally, in this model, flow was controlled using a clamping mechanism on the side of the device that periodically compressed the channels to simulate calf muscle contractions. All together, these examples demonstrate how vascular MPS can be tailored to replicate complex anatomical features by integrating thoughtful microfluidic design, advanced fabrication processes, and functional mechanical components.

**Self-organizing methods: vasculogenesis and angiogenesis.** Self-organizing methods leverage biological processes occurring during vascular development, usually during prenatal stages, including vasculogenesis and angiogenesis. Vasculogenesis refers to the *de novo* formation of a vascular network from a pool of endothelial progenitor cells present in the tissue, while angiogenesis involves the sprouting of new vessels from pre-existing vessels through EC migration.<sup>45</sup> Another related process, known as neovasculogenesis, occurs postnatally, particularly during tissue repairs or pathological conditions.<sup>46</sup> However, neovasculogenesis has not yet been applied in vascular MPS. This process describes the formation of new vessels within an already existing vascular network, typically originating from circulating endothelial progenitor cells.<sup>46</sup>

Vascular MPS based on vasculogenesis consists of ECs embedded within a hydrogel, where they spontaneously form vascular networks over time (Fig. 1E and G). Common designs include 3-,<sup>47-53</sup> 5-,<sup>54-56</sup> or even 6-channel<sup>57</sup> configurations, separated by micropillars. The central region, which houses the vascular network, can take various shapes, such as diamond-shaped<sup>47-49</sup> or rectangular.<sup>51,53,54,57</sup> Side channels serve as medium reservoirs, perfusion channels or may also be embedded with other cell types. Vasculogenesis is most often induced by growth factors secreted by fibroblasts, which are either co-embedded with the ECs<sup>49</sup> or placed in the side channels.<sup>54,55,57</sup> In some studies, cancer cells have been used to initiate vasculogenesis.<sup>48,50</sup> Similarly, fibroblast-free vascular MPS have also been developed, using growth factor-rich media containing vascular endothelial growth factor (VEGF) and fibroblast growth factor (FGF)<sup>47,51-53,56</sup> to induce network formation. These vasculogenesis-based models are particularly valuable for studying interactions between ECs and organ-specific, tumor, or perivascular cells

through direct co-culture within the gel<sup>51,53</sup> or by culturing them on top of the vascular network.<sup>55,56</sup>

Angiogenesis-based vascular MPS designs are often similar or even identical to those used in vasculogenesis-based models. However, in angiogenesis models, the gel-containing region is either lined with ECs that will sprout into the gel<sup>53</sup> or contains a pre-existing vascular network from which sprouts emerge<sup>57</sup> (Fig. 1F and G). Sprouting is stimulated by specific signals such as growth factors,<sup>53,58</sup> fibroblasts,<sup>51,54,55,57,59</sup> or cancer cells<sup>60</sup> embedded within or across the gel. These models are particularly useful to study angiogenic potential in the presence of perivascular cells<sup>51,53</sup> or tumor cells,<sup>60</sup> or the response to physical cues<sup>57</sup> or therapeutic drugs.<sup>57</sup>

In contrast to vasculogenesis and angiogenesis, which are well-characterized and widely used in vascular MPS, neovasculogenesis remains relatively poorly understood and has not yet been implemented in the field. Only a limited number of studies have explored this process, showing its critical roles in tissue repair and pathological conditions.<sup>61</sup> Therefore, the development of vascular MPS models capable of recapitulating neovasculogenesis would provide valuable insights into its underlying mechanisms and functional relevance.

## II.2) Cellular and acellular considerations for physiological relevance

In vascular MPS, the EC source is the most critical factor for achieving physiological relevance, as ECs are the cornerstone of vasculature. Perivascular cells, such as fibroblasts, pericytes, and SMCs, are equally important since blood vessels *in vivo* are composed of multiple cell types, required for their structure, function, and stability. In addition to cellular components, the microenvironment plays a major role in vascular physiology and pathology. Key elements include the basement membrane, which can be mimicked with artificial membranes, and the ECM, which is recreated using hydrogels. Together, these components create a more realistic environment that supports vascular formation, function, and the study of disease models.

**Endothelial cells: umbilical, cell lines, organ-specific, and progenitors.** The source of ECs is a critical factor in constructing *in vivo*-like vasculature and vascularized tissues or organs. Human umbilical vein ECs (HUVECs) are conventionally used in MPS research, both in pre-patterning and self-organizing methods (Fig. 2A), as they are easy to source and culture, and most importantly for their ability to form vascular structure and express genes associated with EC phenotype, notably tight junctions.<sup>54,62-64</sup> HUVECs serve as a versatile tool facilitating studies on vascular development, barrier functions, and responses to chemical stimuli.<sup>58,65,66</sup> In pre-patterning methods, HUVECs are mainly used to investigate barrier functions in interaction with epithelial cells.<sup>29,64,67</sup> In self-organizing methods, they enable the analysis of vasculature morphology over time, including

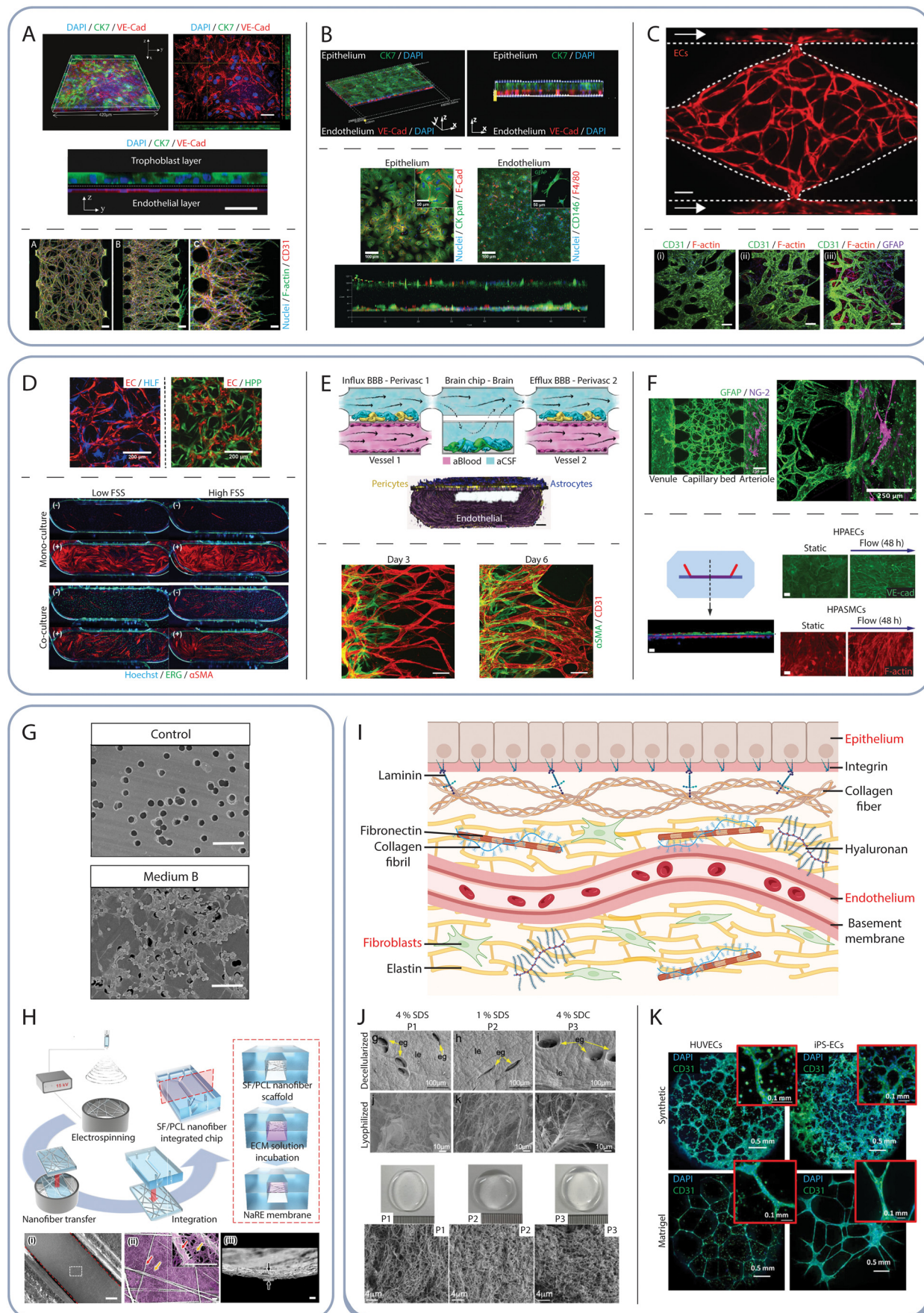


**Fig. 2** Diversity of ECs and perivascular cells, and importance of extracellular components: membrane and matrix in vascular MPS. A) HUVECs are the most commonly used EC type in vascular MPS. Top panel shows a 2D bilayer device composed of a trophoblast epithelium and HUVECs, recapitulating a placental model.<sup>67</sup> Scale bars: 50  $\mu\text{m}$  and 30  $\mu\text{m}$ . The figure has been rearranged from the original. Bottom panel represents both vasculogenesis (A) and angiogenesis (B and C) methods to form a 3D vascular network with HUVECs.<sup>54</sup> Scale bars: 100  $\mu\text{m}$  (A and B) and 50  $\mu\text{m}$  (C). The figure has been rearranged from the original. B) Organ-specific ECs in 2D bilayer models. Top panel illustrates a lung-on-chip model with alveolar epithelial cells (HPAEpiC) and human lung microvascular ECs (HULEC-5a line).<sup>30</sup> Bottom panel displays a liver-on-chip model, encapsulating hepatocytes (left and inset) liver sinusoidal ECs (right), and hepatic stellate cells (right inset) isolated from murine liver samples.<sup>82</sup> Scale bars: 100  $\mu\text{m}$  and 50  $\mu\text{m}$ . The figure has been rearranged from the original. C) Progenitor-derived ECs in 3D vascular MPS. Top panel presents a 3D vascular network derived from ECFC-ECs.<sup>48</sup> Scale bar: 100  $\mu\text{m}$ . Bottom panel is a 3D BBB-on-chip model created using iPSC-ECs monoculture (i), or in co-culture with brain pericytes (ii), or both pericytes and astrocytes (iii).<sup>208</sup> Scale bars: 100  $\mu\text{m}$ . D) Fibroblasts are commonly used as a tool, but rarely are the focus of studies. Top panel shows a 3D HUVEC-based vascular network in contact with human lung fibroblasts (HLF in blue) and human placental pericytes (HPP in green).<sup>68</sup> Scale bars: 200  $\mu\text{m}$ . Bottom panel is a 2D bilayer device with primary human retinal microvascular ECs and dermal fibroblasts, in the presence (+) or absence (-) of 10 ng  $\text{mL}^{-1}$  TGF $\beta$ 1.<sup>97</sup> Channel size: 4 mm  $\times$  1 mm. E) Pericytes are commonly used in contact with ECs. Top panel illustrates a 3-device BBB-on-chip model with brain pericytes.<sup>32</sup> Scale bar: 75  $\mu\text{m}$ . The figure has been rearranged from the original. Bottom panel is a 3D angiogenesis model with dermal pericytes lined to the vessels.<sup>59</sup> Scale bars: 100  $\mu\text{m}$ . The figure has been rearranged from the original. F) SMCs are used to recreate artery or arteriole models. Top panel presents a 3D hierarchical vascular system, encapsulating a venule, capillaries, and an SMC-lined arteriole.<sup>35</sup> Scale bars: 250  $\mu\text{m}$ . The figure has been rearranged from the original. Bottom panel displays a 2D bilayer pulmonary artery-on-chip with pulmonary arterial ECs and pulmonary arterial SMCs, under flow conditions.<sup>31</sup> ECs align parallel to flow, while SMCs align perpendicularly. Scale bars: 10  $\mu\text{m}$ . The figure has been rearranged from the original. G) Scanning electron microscopy (SEM) images from the Transwell membrane without or with coating, composed of fibrinogen and growth factors (medium B).<sup>285</sup> Scale bars: 50  $\mu\text{m}$ . The figure has been rearranged from the original. H) Protocol for the formation of electrospun membranes, composed of SF-PCL fibers and ECM gel.<sup>119</sup> SEM images of the membrane (i, ii, and inset). The red arrow highlights SF-PCL fibers and yellow collagen nanofibrils. iii shows a cross section image of the membrane. Scale bars: 500  $\mu\text{m}$  and 2  $\mu\text{m}$ . I) Schematic of ECM organization. Red words are cellular components, black words are ECM components. Created in BioRender. Fujimoto, K. (2025) <https://BioRender.com/y31y833>. J) SEM images of decellularized (g-i) and lyophilized (j-l) endometrium tissues, following three protocols (P1-3).<sup>157</sup> Scale bars: 100  $\mu\text{m}$  and 10  $\mu\text{m}$ . Gross and SEM pictures of the dECM-derived hydrogels at a concentration of 10 mg  $\text{mL}^{-1}$ . Scale bars: 4  $\mu\text{m}$ . The figure has been rearranged from the original. K) Vascular network derived from HUVECs and iPSC-ECs, out-of-device, using Matrigel or synthetic PEG-based hydrogels.<sup>166</sup> Insets show magnified images of each gel. Scale bars: 0.5 mm and 0.1 mm. All figures have been edited to enhance readability.

parameters such as vascular diameter, connectivity, and length.<sup>54,58,68</sup> Moreover, HUVEC-based self-organizing methods have been used to replicate *in vivo*-like barrier functions and to study drug effects.<sup>66,69</sup> A less commonly utilized EC source is human umbilical artery ECs (HUAECs).<sup>70</sup> Combining HUVECs and HUAECs to create vascular networks allows researchers to model heterogeneous blood vessels, offering new insights into the roles of different EC types in vasculogenic processes.<sup>70</sup>

Similarly, other types of ECs, including EC cell lines and immortalized ECs, have also been used in vascular MPS. Several studies have demonstrated their applicability for modeling vascular functions. For instance, the EC line EA.hy926 was used to construct a liver-on-chip model, in which hepatic functions were successfully maintained under flow conditions.<sup>71</sup> Another example is the use of TeloHAECS, an immortalized human aortic EC line, in a pre-patterned vascular lumen model to evaluate tumor cell intravasations.<sup>72</sup> Both studies highlight the feasibility of incorporating EC cell lines and immortalized ECs into vascular MPS. Overall, these different types of ECs already grant access to meaningful information about vascular development, barrier functions, and interactions with the environment.

However, using non-organ-specific ECs presents some limitations in recreating organ specificity or diseases *in vitro*. Both HUVECs and HUAECs are differentiated cells that express specific phenotypes associated with the umbilical cord.<sup>73</sup> For cell lines and immortalized cells, altered biology and genetic anomalies are often present, compared to *in vivo* cells. Meanwhile, it is well known that ECs have structural specificity and differences among organs: continuous,

fenestrated, and discontinuous ECs.<sup>74</sup> More recent advancements in multi-omics and single-cell RNA sequencing (scRNA-seq) technologies have further revealed significant EC diversity in humans and mice.<sup>75,76</sup> This diversity also extends to pathological responses, as specific EC types react differently to disease conditions. For example, a recent study shows that kidney-derived ECs are more susceptible to diabetes-associated damage than ECs from other organs.<sup>77</sup> These findings emphasize the importance of using organ-specific ECs for constructing vascular MPS. Incorporating organ-specific ECs would enhance physiological relevance, enabling more accurate modeling of both healthy and pathological vascular environments.

Organ-specific microvascular ECs have been used in MPS to model tissue–capillary interactions and investigate organ-specific functions such as barrier integrity and molecular transport, particularly through pre-patterning methods. Continuous ECs, such as those present in the lungs and brain, are crucial for preventing harmful chemicals or pathogens from penetrating blood or tissue. The first MPS, a lung-on-chip, incorporated pulmonary microvascular ECs (HPMECs) to replicate a continuous phenotype.<sup>26</sup> Numerous other studies use different cell lines of human lung microvascular ECs<sup>30,78–80</sup> (Fig. 2B top). Similarly, for brain models, human brain microvascular ECs (HBMECs) have been used to create a continuous and tight blood–brain barrier (BBB) in contact with pericytes and astrocytes, mimicking the *in vivo* environment.<sup>32</sup> In contrast, fenestrated endothelium, essential for selective filtration, is characteristic of organs such as the kidney and small intestine. A model mimicking kidney fenestrated endothelium, using glomerular

microvascular endothelial cells (GMECs), successfully demonstrated caveolae-mediated transendothelial transport, replicating key filtration functions of the glomerulus.<sup>81</sup> Finally, discontinuous endothelium, as found in the liver, facilitates efficient metabolic exchanges. A murine liver-on-chip incorporated liver sinusoidal ECs (LSECs) to recreate this specialized endothelium<sup>82</sup> (Fig. 2B bottom). Additional examples of EC types and their applications in organ-specific MPS are reviewed by Urbanczyk *et al.*<sup>83</sup>

While MPS using pre-patterning methods effectively recapitulate capillary diversity using organ-specific ECs, self-organizing methods have yet to achieve comparable versatility. Among MPS using self-organizing methods, BBB-on-chip has been well explored using brain-specific ECs, with, for instance, Winkelman *et al.* employing primary HBMECs to generate a 3D vessel network.<sup>53</sup> HBMECs display higher mRNA expression of permeability-related genes<sup>51</sup> and better mimic *in vivo*-like permeability compared to HUVECs.<sup>84</sup> Other examples include human dermal microvascular ECs (HDMECs),<sup>55</sup> human colonic microvascular ECs (HCoMECs),<sup>85</sup> and HPMECs.<sup>86</sup> Despite these promising examples, the number of MPS capable of recapitulating 3D, organ-specific microvascular networks remains limited, highlighting a significant gap in modeling the structural and functional diversity of tissue-specific capillaries.

Alternative sources of ECs are progenitor cells and stem cells. Endothelial colony-forming cells derived ECs (ECFC-ECs) and induced pluripotent stem cell-derived ECs (iPSC-ECs) are particularly noteworthy. ECFC-ECs, which are resident cells within the vasculature, can migrate to injury sites and differentiate into specific EC types. They exhibit prolonged replication capacity<sup>87,88</sup> and greater angiogenic potential than HUVECs,<sup>89</sup> making them ideal candidates for self-organizing methods (Fig. 2C top). Similarly, iPSC-ECs can form a perfusable vasculature *via* self-organization and differentiate into organ-specific ECs<sup>51,90</sup> (Fig. 2C bottom). Moreover, iPSC-ECs offer the unique advantage of being sourced from patients with specific diseases, allowing the recapitulation of pathological development and phenotypes.<sup>52,91</sup> This capability makes iPSC-ECs invaluable for creating both healthy and diseased models, advancing research into vascular biology, and opening new opportunities in personalized medicine.

Overall, the choice of EC source is a critical parameter in vasculature studies using vascular MPS. While HUVECs remain widely used in MPS, the field is increasingly adopting alternative cell sources to enhance physiological relevance. Organ-specific ECs and ECFC-ECs both offer substantial potential to enhance the fidelity of vascular models in MPS research. In the context of personalized medicine, iPSCs-ECs and patient-derived ECs represent promising approaches, enabling the generation of personalized, organ-specific vascular networks. One example, explored by Perry *et al.*, utilized patient-derived ECs from the limb veins in an out-of-device model to successfully form a 3D vascular network.<sup>92</sup>

**Perivascular cells: fibroblasts, pericytes, and smooth muscle cells.** While ECs are the primary component of blood

vessels, perivascular cells, such as stromal cells (e.g., fibroblasts) and mural cells (e.g., pericytes and SMCs), are essential for proper vasculature organization and functions.<sup>74,93</sup> Incorporating these supporting cells into MPS is a critical step toward developing more accurate and physiologically relevant models.

*In vivo*, fibroblasts reside within the ECM, playing a key role in ECM remodeling<sup>93</sup> and growth factor secretion.<sup>93–95</sup> Consequently, fibroblasts are frequently used in self-organizing methods to support EC vasculogenesis or angiogenesis (Fig. 2D top), limiting fibroblasts as a simple tool for vasculature formation and overlooking their broader contributions to vascular biology. Meanwhile, crosstalk between ECs and fibroblasts is pivotal in both physiological and pathological contexts. For instance, a recent study demonstrated that fibroblasts can generate physical cues, such as ECM stiffening, which promote vasculogenesis and enhance blood vessel integrity.<sup>96</sup> Another study showed that ECs can alleviate myofibroblast activation mediated by TGF $\beta$  signaling, highlighting crosstalk between these cell types<sup>97</sup> (Fig. 2D bottom). These studies emphasize the importance of exploring fibroblast-EC interactions in MPS, particularly under both normal and pathological conditions. By addressing these interactions, MPS can uncover insights from vascular biology and improve the functionality of engineered vascular MPS.

Mural cells, another type of perivascular cell, are in direct contact with vessels.<sup>93</sup> These include pericytes, which are close to capillaries, and SMCs, which are associated with arteries and veins.<sup>74</sup> Both cell types play crucial roles in maintaining vascular integrity and stability.<sup>98</sup> Pericytes are usually incorporated into MPS to replicate tissue-specific vascular characteristics, especially for lung or brain modeling. As pericytes are critical for maintaining the BBB, numerous studies have encapsulated pericytes *on-chip*<sup>32,51,59</sup> (Fig. 2E). Pericytes allow the recapitulation of capillary-like phenotypes by enabling the formation of smaller-diameter vessels in self-organizing methods.<sup>68,88</sup> Additionally, encapsulating pericytes within vascular MPS allows the modeling of another hallmark of lung or brain capillaries: their reduced permeability. MPS incorporating lung or brain pericytes have successfully achieved this characteristic, further enhancing physiological relevance.<sup>32,59</sup>

SMCs, on the other hand, are used to recapitulate artery-like blood vessels.<sup>31,35</sup> In a pre-patterning method, SMCs can be incorporated into relatively large 3D blood vessels to achieve an *in vivo*-like environment (Fig. 2F top).<sup>35</sup> Another notable example is the development of a three-layer arteriole model, consisting of ECs, SMCs, and fibroblasts, representing the tunica intima, media, and externa, respectively.<sup>99</sup> The authors successfully replicated early-stage atherosclerosis by applying various initiating stimuli, such as low-density lipoprotein (LDL) and tumor necrosis factor  $\alpha$  (TNF $\alpha$ ). The authors investigated vasoactivity, permeability, and monocyte phenotypes, as well as evaluated the efficacy of therapeutic drugs. In a self-organizing model, iPSC-derived SMCs have been utilized to investigate the

interactions between SMCs and vascular structures, focusing on the relationship between SMC spatial localization and contractile function.<sup>100</sup> Alternatively, in more traditional 2D bilayer devices, SMCs are employed to study diseases affecting arterial walls or SMC-specific functions, such as pulmonary arterial hypertension (PAH) (Fig. 2F bottom).<sup>31</sup> Although some vascular MPS incorporating SMCs are already established, further refinement and expanded investigation are warranted, given the critical role of SMCs in vascular physiology and disease.

Like ECs, perivascular cells present heterogeneous and organ-specific gene and protein expression patterns.<sup>101</sup> Advances in multi-omics technologies revealed this diversity both between and within organs.<sup>101–104</sup> Fibroblasts demonstrate inter- and intra-organ heterogeneity across various tissues, including the heart, skeletal muscles, colon, bladder,<sup>101</sup> brain,<sup>102</sup> liver,<sup>103</sup> and kidney.<sup>104</sup> Therefore, fibroblasts from different organs are likely to influence vascular morphology differently, as seen with lung fibroblasts producing larger diameters compared to dermal fibroblasts or bone marrow-derived mesenchymal stem cells.<sup>105</sup> Pericytes have also exhibited organ-specific functionality in vascular MPS. Patient-derived CD90+ CD146+ pericyte-like cells from lung tissues have been used to develop chronic obstructive pulmonary disease *on-chip*.<sup>106</sup> Similarly, both primary and iPSC-derived brain pericytes have been successfully used to construct the BBB,<sup>32,107</sup> highlighting the value of organ-specific pericytes in generating physiologically relevant MPS. Additionally, non-perivascular cells have also been incorporated in vascular MPS, such as astrocytes for brain,<sup>32,51</sup> stellate cells for liver,<sup>82</sup> and mesangial cells for kidney glomeruli.<sup>108</sup> Overall, similarly to ECs, using organ-specific perivascular and non-perivascular cells in vascular MPS is key for improved relevance.

**Membrane: current and future generations.** In 2D bilayer MPS, membranes are key in separating compartments and supporting cell growth. These membranes are designed to mimic the basement membrane found *in vivo*, which separates endothelium from surrounding tissues.

The most widely used membranes are PET porous membranes (Fig. 2G), with pore sizes ranging from 0.4  $\mu\text{m}$  to 8  $\mu\text{m}$  and a thickness of approximately 8–10  $\mu\text{m}$ , making them suitable for a wide range of applications, such as brain,<sup>32,109</sup> lung,<sup>29,31</sup> or placenta models.<sup>67</sup> Other materials are also widely used; for instance, PDMS can be spun into thin layers to create membranes. Notable examples include a 10  $\mu\text{m}$ -thick PDMS membrane used in the original lung-on-chip.<sup>26</sup> Another study uses 25  $\mu\text{m}$  membranes with 5  $\mu\text{m}$  pores for a gut-on-chip model.<sup>110</sup> Polycarbonate (PC) is another frequently used material, offering membranes with a thickness of around 10  $\mu\text{m}$  and pore sizes ranging from 0.4 to 10  $\mu\text{m}$ .<sup>32,111,112</sup> More recently, silicon nitride (SiN) membranes have gained attention in applications such as BBB-on-chip to study particle translocation and transcytosis.<sup>113,114</sup> SiN membranes are exceptionally thin, with a thickness of approximately 100 nm, closer to the <100 nm of the *in vivo* basement membrane.<sup>115,116</sup> These

membranes are highly permeable, capable of sustaining cell culture, and provide superior imaging resolution compared to traditional materials.<sup>113,114</sup>

The membranes previously described present two shortcomings: a higher thickness and a less relevant structural organization compared to *in vivo* conditions. These membranes are typically flat, relatively smooth, and less elastic, whereas the natural basement membrane comprises collagen and other proteins arranged into fibrous, mesh-like sheets that provide elasticity and structural complexity.<sup>116–118</sup> To overcome such shortcomings, electrospun membranes have emerged as a promising alternative. They are thinner (<5  $\mu\text{m}$ ), highly permeable, and composed of fibers resembling *in vivo* bundles with diameters of <100 nm.<sup>119</sup> Electrospun membranes are increasingly used in MPS, particularly for modeling organs subjected to mechanical cues, flow, or stretch. Examples include MPS with integrated vasculature<sup>119,120</sup> (Fig. 2H) and those without vasculature,<sup>121–123</sup> both of which show the elastic properties of these membranes. Broadly speaking, materials range from plastic polymers such as poly(methyl methacrylate) (PMMA)<sup>121</sup> or polycaprolactone (PCL)<sup>119,120,122,123</sup> to biopolymers such as silk,<sup>119,120,124,125</sup> collagen,<sup>123,126</sup> and composites like chitosan.<sup>127</sup> However, in vascular MPS, the combination of both plastic- and biopolymer-based membranes shows great promise, as highlighted in Kanabekova *et al.*,<sup>123</sup> where they use PCL and collagen.

Finally, despite some examples of biopolymer-based membranes, most membranes used in vascular MPS are made of plastic or other synthetic materials. While these membranes are generally biocompatible, their intrinsic material properties continue to limit their ability to fully replicate physiological environments. Key characteristics, including elasticity, permeability, and cell adhesion capability, still fall short when compared to the native basement membrane. Therefore, further advancements in membrane materials and fabrication techniques are necessary to enhance their functional resemblance to *in vivo* conditions and support more physiologically relevant tissue models.

Currently, to compensate for the cell binding capability, numerous studies use a subsequent coating, notable to facilitate cell adhesion and growth, mimicking the composition of basement membrane proteins. The choice of coating agents is diverse and depends heavily on the cell type being used, requiring optimization to find the most suitable match. Collagen<sup>26,31,32,67,110,112–114,119</sup> and fibronectin<sup>26,32,109,113,114</sup> are the two most commonly used coating agents (Fig. 2G). In some cases, specialized coatings are employed to cater to specific cell types. For example, Yadav *et al.* used iMatrix-511 for airway chips and Geltrex for alveoli chips, to match the sensitivity and specificity of each iPSC-derived cell.<sup>29</sup> Typically, the choice of coating agent is guided by a combination of trial-and-error and previous literature, making it a case-dependent parameter.

**Matrix: convention, alternative, and perspective.** In 3D devices, the ECM plays a major role in device design for vessel development. The vascular ECM is a complex network of

proteins and carbohydrates, providing structural support and regulating cellular functions *via* signaling molecules, such as cytokines and growth factors.<sup>128</sup> The ECM also supports the formation and maintenance of vascular networks<sup>129</sup> by facilitating EC proliferation, migration, and adhesion, through biochemical and mechanical cues.<sup>130</sup> Additionally, the vascular ECM is involved in various pathologies, most notably fibrosis and cancer.<sup>131</sup> These diverse properties make the ECM a crucial component for developing physiologically and pathologically relevant vascular MPS.

*In vivo* vascular ECM encapsulates multiple components, such as proteins, glycoproteins, and polysaccharides (Fig. 2I). Proteins include collagen, the most abundant and ubiquitous component, which provides structural support and tensile strength to blood vessels;<sup>132</sup> elastin, which is responsible for elasticity, particularly in artery walls;<sup>132,133</sup> and laminins, which are important for the structure and function of the basement membrane.<sup>132,134</sup> Glycoproteins include proteoglycans, which maintain structural integrity and regulate the availability of growth factors, cytokines, and water,<sup>135,136</sup> and fibronectin, which serves as a critical linker between the ECM and cells.<sup>137,138</sup> Lastly, glycosaminoglycans, such as hyaluronic acid, are the main polysaccharides contributing to the ECM's hydration and structural properties.<sup>135,139</sup> However, due to technical limitations, replicating the exact composition of the *in vivo* ECM remains challenging *in vitro*. In vascular MPS, the ECM has been widely mimicked using fibrinogen and collagen, with additional alternatives such as gelatin, alginate, and Matrigel being widely employed.

Fibrinogen is one of the most used ECM components in vascular MPS.<sup>51,52,62,68,70,84,87,88</sup> The standard protocol requires fibrinogen to be cleaved into fibrin using thrombin, which then polymerizes into a gel to support lined or embedded cells. Despite fibrinogen being prevalent, collagen type I remains another frequently employed ECM component in MPS.<sup>63,90,140,141</sup> Collagen protocols typically require pH neutralization and temperature-dependent polymerization to generate stable gels. Some studies have combined both fibrinogen and collagen to leverage their complementary properties.<sup>54,65,142,143</sup> The final concentration of each component is case-dependent and influenced by various parameters such as cell type, vascularization method, and experimental outcomes. For fibrinogen, concentrations usually range between 2 and 10 mg mL<sup>-1</sup>, while collagen concentrations vary between 2 and 6 mg mL<sup>-1</sup> when used alone and around 0.2 mg mL<sup>-1</sup> when mixed with fibrinogen. Helm *et al.* showed in an out-of-device model that both fibrinogen and collagen concentrations impacted vascular network development.<sup>144</sup> Similarly, Whisler *et al.* showed in an *on-chip* study that increasing fibrinogen concentration enhanced network branching, with the branch surface area increasing proportionally.<sup>62</sup> Overall, fibrinogen and collagen are the most widely used hydrogels to mimic the ECM in vascular MPS, despite their relatively limited relevance.

To achieve greater physiological relevance, animal-derived gels are also employed. Gelatin, a collagen-rich material derived from animal tissues, can be used alone or in combination with other components, such as polyethylene glycol (PEG) or methacrylic anhydride (MA). For instance, gelatin-MA has been used to embed cells in a 2D bilayer device,<sup>145</sup> while gelatin with or without PEG has been used to generate a lumen scaffold in a 3D pre-patterning method.<sup>146</sup> Another common option is Matrigel, a native basement membrane matrix derived from the Engelbreth-Holm-Swarm mouse tumor. Matrigel is rich in laminin, collagen IV, and growth factors, making it highly effective in promoting angiogenesis and vascularization.<sup>147</sup> While Matrigel is commonly used for organoid and spheroid formation, Matrigel has also been successfully applied in MPS studies.<sup>148-150</sup>

One of the most promising alternatives is decellularized matrix (dECM). Derived from native tissues, dECM can originate from various species (human, rat, mouse, pig) and organs (lung, brain, liver, kidney). Decellularization processes remove cellular components while preserving the ECM components and structures.<sup>151-153</sup> This is achieved using a combination of chemical methods (detergents such as Triton X-100, SDS, hyper-/hypotonic solutions), enzymatic methods (trypsin or nuclease), and physical methods (freeze-thaw cycles, sonication, scraping, or ultra-high pressure). Most protocols combine these approaches to ensure effective cell removal while maintaining ECM integrity. Following decellularization, dECM can be used as a scaffold for tissue culture and engineering,<sup>151</sup> or reduced into powder form to create hydrogels.<sup>152-154</sup> Subsequent hydrogels have been applied in cancer modeling,<sup>154</sup> organoid culture<sup>153,155-159</sup> (Fig. 2J), and MPS.<sup>160-164</sup> In MPS, dECM has primarily been utilized to study organoid development,<sup>155</sup> skin aging,<sup>162</sup> or anti-cancer drug efficiency,<sup>160,163,164</sup> but has not yet been adopted for vascular studies. Despite the availability of commercially produced dECM,<sup>165</sup> its broader application remains limited by challenges related to ethical considerations and sample availability, as dECM is derived from animal or human tissues. For this reason, its use in vascular MPS is currently limited. However, several avenues exist for its application in vascular MPS, such as testing commercially available materials, fostering collaborations between researchers and clinicians to source tissue ethically, or leveraging future advancements in the dECM field. Nevertheless, due to its high physiological relevance and versatility, dECM holds strong potential as a biomimetic material for vascular research in MPS.

Lastly, synthetic gels, including PEG and polyacrylamide, have gained attention as alternatives to natural gels. These materials offer advantages such as well-defined composition, reproducibility, and stable mechanical and biochemical properties. Nguyen *et al.* highlighted the superior consistency of PEG compared to Matrigel, showcasing its potential for EC culture and vascular modeling, in an *out-of-chip* model<sup>166</sup>

(Fig. 2K). Additionally, HUVECs have been shown to form vascular networks within a PEG-containing device.<sup>167</sup>

### III. Vascular MPS as potent tools

#### III.1) Recapitulation and study of vascular physical aspects

Vascular MPS enable precise reproduction and investigation of various physical parameters that influence vascular function. *In vivo*, blood vessels are constantly exposed to mechanical forces arising from hemodynamic activity, such as shear stress and interstitial flow. These forces are essential not only for vascular development and homeostasis but also play significant roles in the progression of vascular pathologies. Furthermore, the vasculature is responsible for the exchange of gases, nutrients, and waste products, while simultaneously acting as a selective barrier that prevents the infiltration of harmful substances. This selective transport is governed by endothelial permeability, another crucial parameter that can be studied using vascular MPS.

**Luminal flow: shear stress or static.** Fluid shear stress is one of the most extensively studied mechanical cues in vascular MPS. *In vivo* experiments have been implemented and revealed a strong coupling between shear stress and physiological or pathological processes, such as atherosclerosis or atheroma formation.<sup>168,169</sup> Leveraging these insights, vascular MPS has been intensively used to study shear stress, thanks to the inherent channel-based fluidic designs. By controlling geometry and flow rate, vascular MPS can replicate *in vivo*-like conditions with high fidelity.

Shear stress can be applied across various MPS types, including 2D bilayer devices,<sup>31,170–172</sup> 3D models based on pre-patterning methods,<sup>173</sup> and self-organizing 3D vascular networks.<sup>142</sup> In both 2D and 3D systems, exposure to shear stress induces alignment of ECs to the flow direction, both in their overall orientation and cytoskeleton organization, mimicking *in vivo* EC behavior in blood vessels<sup>174,175</sup> (Fig. 3A). SMCs also respond to shear stress by aligning perpendicularly to the direction of flow.<sup>31</sup>

In 3D self-organizing vascular MPS, the effect of flow and shear stress on angiogenic sprouting remains controversial.<sup>141,173,175,176</sup> Some studies show that shear stress inhibits angiogenesis<sup>141,175</sup> (Fig. 3A), whereas another study suggests that angiogenesis may be triggered only after a specific shear stress threshold.<sup>173</sup> A possible explanation, proposed by Wragg *et al.*,<sup>176</sup> is that angiogenesis is not triggered by shear stress itself, but rather by changes in shear stress within the vascular network. The timing of flow initiation and the magnitude of variation between baseline and flow conditions may, therefore, result in divergent outcomes. These contradictory findings emphasize the need for further exploration of shear stress and its relationship with angiogenesis. When it comes to vasculogenesis, shear stress has also been associated with the enhancement of network expansion, as evidenced by an increased number of branches, junctions, and endpoints.<sup>142</sup> Shear stress has also been shown

to modulate mRNA and protein expression in ECs, including upregulation of endothelial nitric oxide synthesis (eNOS), a hallmark of EC function highly linked to shear stress,<sup>176</sup> as well as other markers such as thrombomodulin<sup>170</sup> and angiotensin-converting enzyme 2 (ACE2).<sup>177</sup>

Despite its importance, many MPS studies overlook the incorporation of flow and shear stress, often opting for static conditions. This may be attributed to a lack of reference values for *in vivo* blood flow rates and shear stresses, as well as the challenges associated with quantifying shear stress within devices. Computational simulations can be used to address these challenges, either by determining the precise flow rates required to achieve a target shear stress<sup>31,175</sup> (Fig. 3B) or by retrospectively analyzing the flow conditions applied.<sup>142</sup> Real-time measurements in microfluidic channels can also help evaluate the flow rate and shear stress more accurately.<sup>178</sup>

Overall, the development of flow generation systems has further expanded the applicability of shear stress in MPS. To date, syringe pumps<sup>142,173,175</sup> and peristatic pumps<sup>31,170,174,175</sup> have been commonly utilized to generate flow. These devices are relatively affordable and readily accessible; however, they often require complex experimental setups involving extensive tubing and bubble traps. Alternative methods, such as pressure-driven flow or magnetic stirrers, have also been used.<sup>179</sup> While these methods are simpler to implement and require less intricate setups, they usually offer limited control over the flow rate and may struggle to maintain stable, continuous flow. Improvements have, however, been achieved in a pressure-driven method by incorporating pumps and pressure sensors to maintain a constant pressure difference.<sup>180</sup> More recently, applications of oscillatory flow systems using a piezoelectric pump<sup>171</sup> or pneumatic pressure<sup>172</sup> showcase the potential for more precise and reproducible control of fluidic conditions. These systems offer improved precision and reproducibility in controlling fluid dynamics within MPS. Given the importance of luminal flow and shear stress in vascular biology, continued development of innovative flow generation strategies is essential to facilitate more physiologically relevant studies and to fully realize the potential of vascular MPS.

**Other flows: interstitial and transluminal flow.** Interstitial flow (IF) refers to the slow, pressure-driven movement of fluids through the ECM and interstitial spaces surrounding blood vessels. IF facilitates the transport of nutrients, waste, and signaling molecules to peripheral cells. Beyond its transport role, IF is now known to play a crucial role in vascular morphogenesis, including tumor angiogenesis, by influencing the distribution and activity of growth factors.<sup>181</sup> To mimic the intricate physical environment associated with IF, 3D MPS models have been used to apply flow within channels and across the ECM, notably using hydrostatic pressure<sup>182</sup> (Fig. 3C).

One of the key findings from MPS studies is that IF promotes angiogenesis,<sup>53,57,183</sup> with a notable sensitivity to the flow direction (Fig. 3D). For instance, vascular sprouting is enhanced when flow is directed from the ECM towards the vessel.<sup>57</sup> More recently, the role of IF on vasculogenesis and

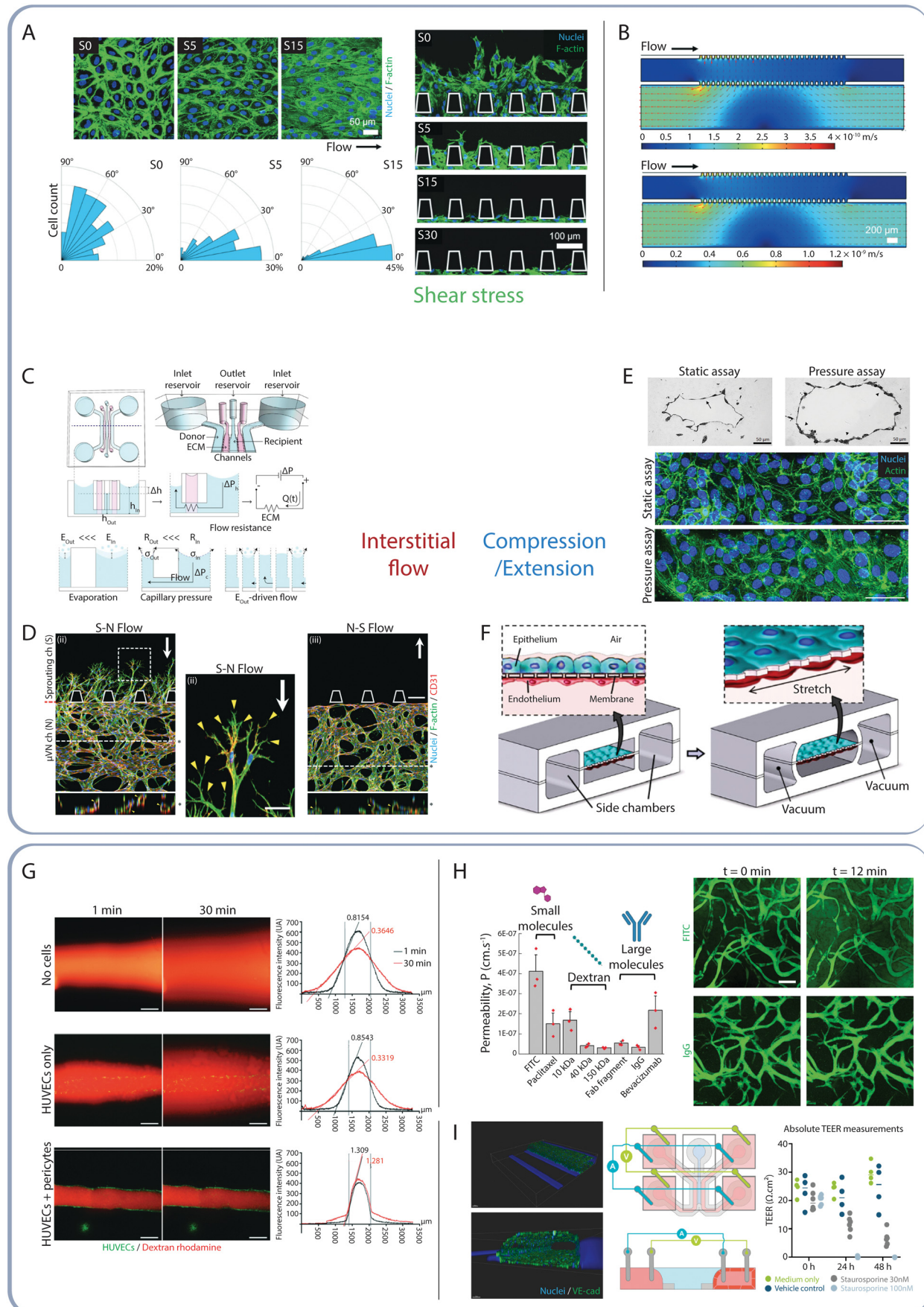


**Fig. 3** Physical aspects in vascular MPS, to study flow, stresses and permeability. A and B) Studies of shear stress in vascular MPS. A) Effect of flow and shear stress on the EC monolayer and angiogenic sprouts.<sup>175</sup> Both EC monolayer alignment to flow and sprouting inhibition increase proportionally with shear stress. Scale bars: 50  $\mu\text{m}$  and 100  $\mu\text{m}$ . The figure has been rearranged from the original. B) Fluid simulation of the device to assess flow velocity applied to the gel with shear stresses of 5 dynes per  $\text{cm}^2$  (top) and 15 dynes per  $\text{cm}^2$  (bottom).<sup>175</sup> Scale bar: 200  $\mu\text{m}$ . The figure has been rearranged from the original. C and D) Studies focusing on interstitial flow. C) Device setup to generate hydrostatic pressure induced by the difference in medium level.<sup>182</sup> The  $\Delta P(t)$  remains around 5 Pa, generating 10  $\text{pL h}^{-1}$  flow corresponding to a 0.015  $\mu\text{m s}^{-1}$  velocity. D) Effect of interstitial flow and direction on angiogenesis.<sup>57</sup> Flow towards sprouts (S-N flow) improves sprouting (ii), while flow from the sprouts (N-S flow) inhibits angiogenesis (iii). Scale bars: 200  $\mu\text{m}$ . The figure has been rearranged from the original. E and F) Compression and extension effects on vascular MPS. E) Intraluminal pressure effect on lumen morphology and cell structure.<sup>189</sup> A pressure of 100 Pa generates an inflated vessel and a change of actin morphology, into a stress fiber phenotype. Scale bars: 50  $\mu\text{m}$ . F) Original lung-on-chip model with stretch modeling.<sup>26</sup> Vacuum is applied to the side chambers, generating a stretch of the central channel and attached cells. G-I) Permeability assessment in vascular MPS. G) Permeability assay in a lumen structure lined with no cells, HUVECs, or HUVECs and pericytes.<sup>198</sup> Dextran rhodamine (70 kDa) has been used over a course of 30 min. Leakages from the lumen to the surrounding ECM highly decrease when lined with both cell types. Scale bars: 500  $\mu\text{m}$ . H) Permeability assay using small- to large-sized molecules in a 3D vascular network over a 12-minute course.<sup>197</sup> Permeability decreases inversely to molecule size. Scale bar: 100  $\mu\text{m}$ . I) TEER method for evaluating endothelium permeability over 48 h exposure to a drug (staurosporine).<sup>200</sup> Staurosporine disrupts the endothelial barrier. Scale bar: 100  $\mu\text{m}$ . All figures have been edited to enhance readability.

organ-specific vascular organization has been studied, primarily in BBB models. Two studies demonstrated improved vascular bed formation and enhanced perfusability under IF conditions,<sup>53,184</sup> with one also showing elevated EC marker expression and cellular alignment perpendicular to the direction of flow.<sup>184</sup> Similarly, Zhang *et al.* established two 3D self-organizing models to investigate the molecular mechanisms underlying IF-mediated vasculogenesis.<sup>185</sup> They found that matrix metalloproteinase-2 (MMP-2) was upregulated in response to IF and further explored their interactions in vasculogenesis in both HUVEC- and HBMEC-based models.

In addition to IF, another flow type is emerging in the vascular MPS field: transluminal flow.<sup>186,187</sup> Offeddu *et al.* focused on the effects of transmural flow on molecular transport across the endothelial barrier, demonstrating that the flow closely mimics *in vivo*-like interstitial transport and varies according to molecular size and properties (protein *vs.* non-protein).<sup>186</sup> Meanwhile, Wang *et al.* showed that transendothelial flow not only enhanced angiogenesis of lined ECs but also promoted anastomosis with pre-existing vascular networks.<sup>187</sup> These studies are examples leading the way in the exploration of transluminal flow and its effect on vasculature processes.

**Compressive/extensive forces: pressure and stretch.** While shear stress and interstitial flow have been in the spotlight, other mechanical cues have also been explored using vascular MPS. Intraluminal pressure is one of the mechanical cues that is thought to play a critical role in regulating *in vivo* vascular environment, but remains poorly understood. Vascular MPS provides a promising avenue for elucidating unanswered questions about intraluminal pressure, highlighted by the study by Offeddu *et al.*,<sup>186</sup> where a 1–2 kPa intraluminal pressure generates a transmural flow and subsequent interstitial flow. Static pressure is another mechanical factor of interest, although it has been less frequently studied. Studies have shown that a static pressure of 200 Pa (1.5 mmHg) inhibits angiogenesis,<sup>188</sup> whereas a pressure of 100 Pa has been found to enhance transendothelial transport and induce vascular morphological changes<sup>189</sup> (Fig. 3E).

Additionally, the stretch of the endothelium is also of interest, as first highlighted in the landmark lung-on-chip study by Huh *et al.*<sup>26</sup> (Fig. 3F). Since that breakthrough, several vascular MPS setups using mechanical or pneumatic actuation systems have been developed, aiming to replicate and study endothelium stretching.<sup>190,191</sup>

**Permeability: assessment methods and applications.** The permeation of molecules across blood vessel walls is crucial for the transport of nutrients and signaling molecules from the blood to surrounding tissues. Therefore, permeability has been of strong interest as an essential parameter for assessing the functionality of vasculature models, both *in vivo* and *in vitro*. Organ-specific variations in vascular permeability can be linked to endothelium types, with fenestrated vessels in the kidneys or discontinuous vessels in the liver exhibiting high permeability, whereas the BBB is characterized by lower permeability.<sup>192</sup> Additionally, enhanced vascular permeability is often observed under inflammatory conditions,<sup>193</sup> underscoring its relevance in pathological contexts. These elements emphasize that permeability is a key parameter to evaluate vascular systems *in vitro*.

In the context of vascular MPS, permeability is a critical criterion for assessing the formation and functionality of vascular networks. The most widely utilized method for assessing permeability is measuring the transport of fluorescent molecules across the endothelial layer. This method is applicable for both 2D bilayer<sup>194,195</sup> and 3D vessel formats.<sup>66,196,197</sup> In 2D devices, permeability is typically measured by analyzing the passage of molecules from one channel to the other, offering the advantages of higher throughput and reproducibility.<sup>195</sup> In contrast, 3D devices evaluate permeability by measuring the leakage of molecules from the vascular lumen to the surrounding microenvironment. Despite being more technically challenging and presenting a lower throughput, 3D formats enable the recapitulation of more complex microenvironments, with structures involved in permeability modulation *in vitro*, such as lumen lined with pericytes<sup>198</sup> (Fig. 3G) or BBB composed of ECs in contact with astrocytes and pericytes<sup>197</sup> (Fig. 3H). Another widely used method for assessing permeability is trans-endothelial electrical

resistance (TEER). TEER measures barrier integrity by quantifying the electric current passing through the endothelial layer.<sup>199</sup> This method offers benefits such as higher time resolution, smaller experimental footprints compared to fluorescence methods, and potential scalability toward high throughput measurement<sup>107,200,201</sup> (Fig. 3I).

Permeability assays have been employed to investigate the effect of chemical, physical, or biological cues on the vasculature. Cytokines and other biochemical stimuli have been used to model vascular responses under inflammatory and infectious conditions.<sup>38,202–205</sup> For example, Fengler *et al.* developed an iPSC-derived microvascular model to assess changes in permeability following IL-1 $\beta$  treatment, identifying anti-inflammatory compounds.<sup>38</sup> Similarly, Faley *et al.* proposed an airway-on-chip for SARS-CoV-2 studies, correlating permeability changes with viral load and other physiological readouts.<sup>206</sup>

Additionally, permeability in relation to other cell types or the microenvironment has also been a focus of numerous studies. In a blood-retinal barrier model *on-chip*, where retinal pigment epithelium and endothelium interact, permeability was assessed under varying degrees of epithelium injury.<sup>207</sup> This study demonstrated that permeability increases with prolonged exposure to reactive oxygen species (ROS)-induced injury. Other studies focused on the impact of fibroblasts<sup>203</sup> and pericytes<sup>142,198</sup> on permeability. Among vascular MPS, the BBB remains the most extensively studied using permeability assessments. BBB models typically incorporate ECs, pericytes, and astrocytes to mimic *in vivo*-like reduced permeability,<sup>107,197,208</sup> providing insights into the intricate interplay between these cell types and their role in maintaining barrier integrity.

Overall, despite their widespread use, permeability assays face several technical challenges. Fluorescence-based assays can be cytotoxic or lead to residual signals, making it difficult to follow the evolution of permeability throughout an experiment. Additionally, 3D permeability assessment mostly relies on quantification based on images, which is less direct and potentially more prone to bias than direct absorbance-based quantifications. On the other end, electrical methods such as TEER may suffer from reproducibility issues and geometric constraints, particularly when adapted to 3D formats. Emerging technologies address these limitations. For example, automated image analysis tools, such as macros, can reduce user bias in fluorescence-based assays.<sup>197</sup> Additionally, the use of electroactive tracers offers a promising hybrid approach that combines the benefits of molecular diffusion and electrical measurement.<sup>194</sup> These continued progresses for permeability assessment provide new avenues for more precise evaluations and more versatile applications.

### III.2) Studies and applications for biomedical prospects

Vascular MPS offer remarkable versatility, making them a powerful tool for exploring biomedical applications. Initially

designed to mimic tissues and organs, these systems have advanced considerably over time. With the growing interest in spheroids and organoids, efforts to integrate these models into vascular MPS have expanded, enhancing their physiological relevance. Importantly, vascular MPS are not limited to replicating healthy conditions; they have also become invaluable tools for studying vascular diseases and cancer, as well as for more biomedical aspects such as immunity, therapy, and drug screening.

**Tissue modeling: interface and organ-like structures.** MPS based on pre-patterning methods have been developed to model various human organs, for example models of lungs,<sup>26,79</sup> liver,<sup>209</sup> and kidneys,<sup>210,211</sup> with a focus on the interactions between endothelium and epithelium (Fig. 4A). Meanwhile, in the field of MPS based on self-organizing vascular methods, the BBB-on-chip is currently of major interest, with models integrating ECs, pericytes, and astrocytes<sup>197,208,212</sup> to mimic the complex microenvironment of the BBB (Fig. 4B).

Tissue modeling has been central to MPS development since the inception of OoC technology. However, a new frontier emerges combining organoids and 3D organ modeling in MPS to create functionally vascularized human organoids. Organoids, widely used in biomedical research, recapitulate human organ structural and morphological features, as well as disease conditions *in vitro*.<sup>213,214</sup> These systems are developed using classical cell lines, primary cells, or increasingly iPSCs.<sup>215</sup> Despite their ability to accurately mimic human organ structure, organoids face critical limitations due to the absence of well-defined vascular networks.<sup>215–217</sup> Without perfusable vasculature, nutrient and oxygen delivery to the inner regions of organoids is restricted, resulting in size limitations and necrotic cores. Furthermore, the lack of functional perfusable vasculature diminishes their potential use as drug screening platforms. *In vivo* transplantation of organoids has successfully induced vascularization,<sup>218,219</sup> however, efforts are now focused on overcoming these limitations *in vitro* by leveraging MPS technologies to vascularize organoids.

When discussing vascularization in MPS, we will classify organoids into two categories: spheroids and proper organoids. Spheroids are aggregates of either healthy or tumor-derived cells – usually cell lines or primary cells – aggregated in a disorganized structure, which can be mixed with other cell types (ECs, fibroblasts, *etc.*). Proper organoids are composed of healthy cells derived from pluripotent stem cells and exhibit organized organ-like structures. Spheroids are generally easier to vascularize by mixing target cells and ECs, aiming to promote anastomosis with pre-existing vascular networks or angiogenic sprouts. For instance, Jin *et al.* generated hepatic spheroids by co-culturing induced hepatic cells with HUVECs, achieving an even higher degree of vascular development when exposed to flow<sup>220</sup> (Fig. 4C). Similarly, Bonanini *et al.* successfully obtained two types of vascularized hepatic spheroids *on-chip*, with vasculature

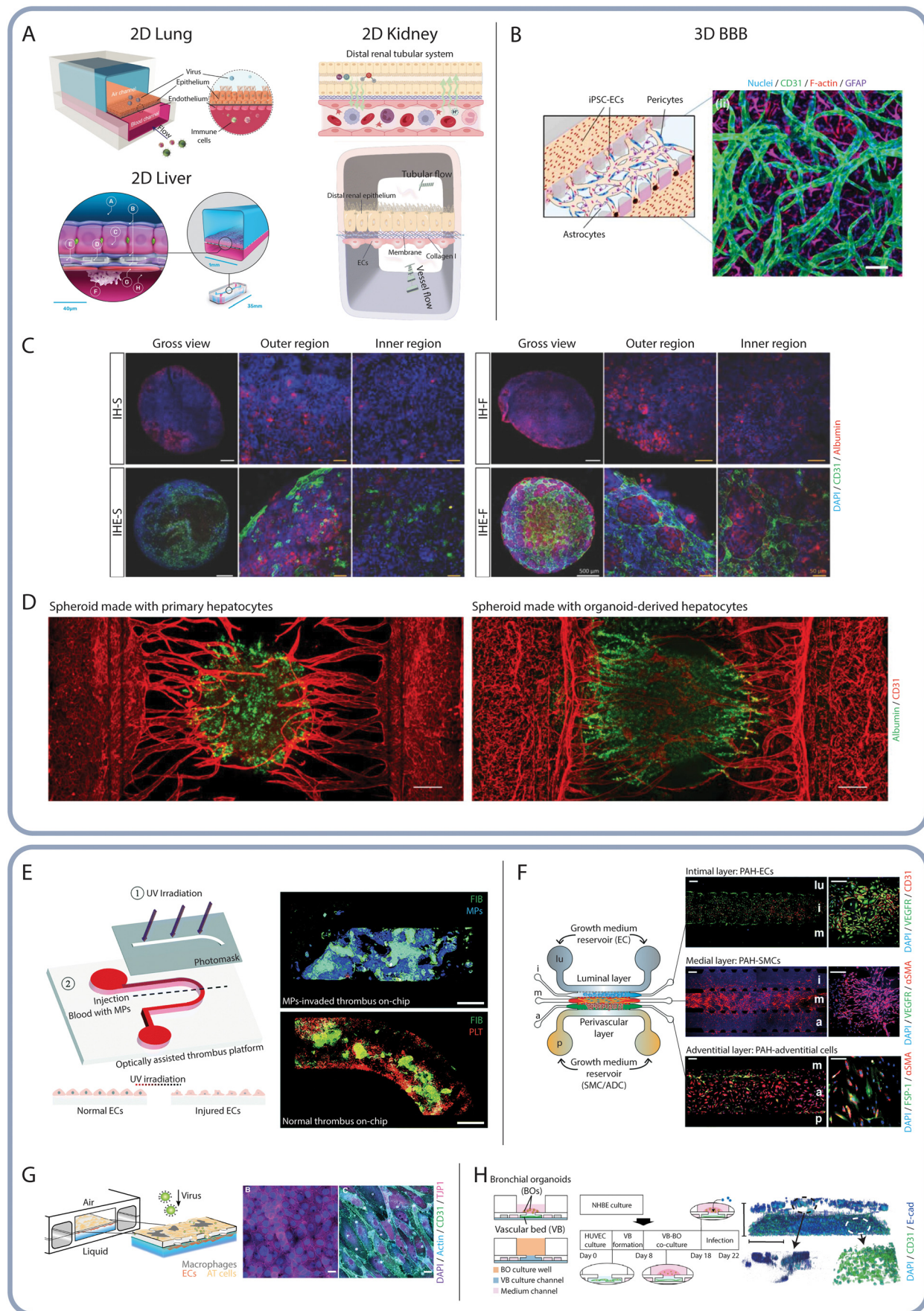


**Fig. 4** Vascular MPS for tissue modeling and organ development. A) Schematics of various 2D bilayer models such as lung-, liver- and kidney-on-chip co-culturing organ-specific epithelial tissue and ECs.<sup>79,209,211</sup> B) Vascular bed *on chip* schematic and confocal image. hiPSC-derived ECs, brain pericytes, and astrocytes formed a vascular network (ii), recapitulating the *in vivo* 3D interface of the human BBB.<sup>208</sup> Scale bar: 100  $\mu$ m. C) Induced hepatic (iHep) cells were cultured with or without HUVECs (iHE or iH), under static or flow conditions (iHE-S/iH-S or iHE-F/iH-F), producing a vascularized organoid-like tissue.<sup>220</sup> White scale bars: 500  $\mu$ m, yellow scale bars: 50  $\mu$ m. D) Vascularized hepatic spheroids made of primary hepatocytes and HUVECs (left) and fetal primary hepatocytes from hepatic organoids (right), using an angiogenesis method.<sup>140</sup> Scale bars: 200  $\mu$ m. E) Thrombosis-on-chip model mimicking injury-induced thrombosis, using whole blood and microparticles.<sup>228</sup> Scale bars: 50  $\mu$ m. F) PAH-on-chip encapsulating pulmonary arterial ECs, SMCs, and adventitial cells, organized in a three-layer configuration.<sup>235</sup> Scale bars: 250  $\mu$ m and 100  $\mu$ m. The figure has been rearranged from the original. G) 2D bilayer device recapitulating endotheliitis and vascular damage after SARS-CoV-2 infection.<sup>78</sup> B and C are the epithelial and endothelial layers, respectively. Scale bars: 20  $\mu$ m. H) Vascular network-bronchial organoid *on-chip* used to mimic vascular damage induced by infected lung epithelium paracrine signaling.<sup>56</sup> Scale bars: 500  $\mu$ m. The figure has been rearranged from the original. All figures have been edited to enhance readability.

infiltrating the spheroids<sup>140</sup> (Fig. 4D). One method involved combining primary hepatocytes with HUVECs, while the other consisted of generating hepatic organoids from fetal primary cells, dissociating them, and reaggregating the cells into spheroids without EC mixing. Other studies have also demonstrated vascularization in cortical<sup>221</sup> or liver<sup>222</sup> spheroids, even in the absence of direct combination with ECs.

In contrast, vascularizing proper organoids *in vitro* remains more challenging. Achieving functional vascular integration often requires extensive optimization, including synchronization of co-culture timing, selection of appropriate supporting cell types, and modulation of biochemical and physical cues.<sup>217</sup> For many organ systems, generating fully perfusable and functional vasculature within proper organoids is still an unmet goal.<sup>216</sup> However, recent progress has identified potential molecular targets to support vascular development. For example, Shaji *et al.* identified CYR61 and HDGF as promising regulators of vascularization in cerebral organoids, offering new strategies to improve vascularization *in vitro* perfusion and maturation.<sup>205</sup> Together, these efforts highlight the increasing potential of MPS platforms to overcome vascularization challenges in both spheroid and proper organoid models, moving the field closer to fully functional, physiologically relevant tissue constructs.

**Vascular diseases: specific and non-specific to the vasculature.** MPS have proven to be powerful tools for studying vascular diseases, affecting either an organ, blood, the vasculature itself, or a combination.<sup>223</sup> Pathologies related to blood and vasculature, such as thrombosis and hypertension, have been explored using vascular MPS. Moreover, despite the existence of vascular-specific diseases, the endothelium can also be altered by pathologies specific to neighboring tissues. The example of viral infections has successfully highlighted the effect of infections on vasculature, using organ-specific vascular MPS.

Thrombosis is the aggregation of platelets, red blood cells, and fibrin within blood vessels and poses a significant risk for heart attacks and strokes if unresolved. Thrombosis-on-chip models have been developed for disease modeling and anti-coagulant drug screening.<sup>40,224-228</sup> For example, Barrile *et al.* demonstrated thrombus formation triggered by an anti-CD154 monoclonal antibody,<sup>226</sup> while Chen *et al.* showed the induction of thrombosis due to microplastic exposure in a

vascular MPS model<sup>228</sup> (Fig. 4E). Outside of PDMS soft lithography MPS, advancements in 3D printing and bioprinting technologies have had a huge impact for thrombosis-on-chip modeling, enabling a more accurate vessel architecture in devices.<sup>229,230</sup>

Hypertension is characterized by elevated blood pressure, defined clinically as a systolic blood pressure (SBP) higher than 130 mmHg and a diastolic blood pressure (DBP) exceeding 80 mmHg.<sup>231</sup> Histologically, hypertension is associated with vascular remodeling, which typically manifests as inward and hypertrophic changes, involving a reduction in luminal diameter due to SMC hyperplasia and hypertrophy within the tunica media.<sup>232,233</sup> Despite the global burden of hypertension, vascular MPS models remain relatively limited, with a few examples focused on PAH. PAH specifically affects pulmonary arteries, defined by a mean pulmonary arterial pressure (mPAP) above 20 mmHg, and is similarly characterized by vascular remodeling.<sup>234</sup> Two studies have successfully recapitulated PAH-related wall thickening and muscularization using MPS. Al-Hilal *et al.* developed a three-layer PAH model incorporating ECs, SMCs, and adventitial cells to mimic the tunica intima, media, and externa, respectively<sup>235</sup> (Fig. 4F). They applied flow-induced mechanical stress and succeeded in reproducing vascular remodeling features such as wall thickening and muscularization. In parallel, Ainscough *et al.* used a two-layer PAH model, using ECs and bone morphogenetic protein receptor type II (BMPR2)-mutated SMCs, combined with hypoxia.<sup>31</sup>

Beyond hypertension and thrombosis, other vascular pathologies have also been explored using MPS, including arteriovenous malformation (AVM)-on-chip<sup>236</sup> and atherosclerosis-on-chip,<sup>237</sup> further emphasizing the potential of vascular MPS to study both vascular-specific and vascular-involved diseases in controlled environments. Additionally, while 2D bilayer devices are widely used to emulate viral infections targeting epithelial cells,<sup>238</sup> recent studies have shown that viral infections can affect the vasculature in addition to their primary organ targets, notably SARS-CoV-2.<sup>239</sup> In 2D device studies, a few models successfully highlight the immune response activation in ECs mediated by signals from SARS-CoV-2-infected epithelial cells<sup>78,240</sup> (Fig. 4G). A similar study has also revealed region-specific EC immune responses in influenza virus-infected

respiratory tracts.<sup>29</sup> Furthermore, a few 3D models have replicated similar immune and vascular responses after SARS-CoV-2 infection, including lung-on-chip<sup>56</sup> (Fig. 4H) and heart-on-chip<sup>241</sup> models.

**Cancer: tumor vasculature and metastasis.** Tumor-induced angiogenesis and vascularization are major hallmarks of cancer development.<sup>5,6</sup> To achieve angiogenesis, cancer cell lines can be used to generate growth factor gradients and enhance sprouting. For example, the glioblastoma cell line (U87MG) has been shown to produce VEGF, effectively inducing angiogenesis.<sup>242</sup> Once established, tumor vasculature differs markedly from healthy vascular networks, exhibiting increased heterogeneity, abnormal permeability, multidirectional flow, and disorganized distribution.<sup>243</sup> Accurately modeling tumor vasculature is therefore key for developing functional *in vitro* tumor models.<sup>244</sup>

The vascularization of tumor spheroids has recently gained momentum in the MPS field.<sup>69,245–247</sup> Nashimoto *et al.* engineered a perfusable and vascularized tumor spheroid by co-culturing HUVECs, breast cancer cells (MCF-7 line), and human lung fibroblasts.<sup>69</sup> Vascularization was achieved by spheroid-induced angiogenesis directed toward the spheroid, followed by anastomosis, as confirmed by immunostaining and histological analysis. Additionally, the anti-cancer effects of paclitaxel on both the spheroid and vasculature were assessed. Two other studies focused on alveolar soft part sarcoma (ASPS) also achieved intra-spheroid vascularization by inducing angiogenesis directed toward the spheroid<sup>245,246</sup> (Fig. 5A). Alternatively, vasculogenesis methods can be used to generate surrounding vasculature, which would then penetrate the spheroids. Straehla *et al.* generated a vascularized glioblastoma by co-culturing a tumor spheroid and a BBB vascular network, exploring permeability and drug therapy considerations.<sup>247</sup> In contrast, Haase *et al.* developed a model in which tumor spheroids were encapsulated within a vascular MPS, focusing not on intra-spheroid vascularization but on the tumor-specific vasculature signature.<sup>248</sup> This approach emphasized the tumor microenvironment and its drug-resistance properties. It is noteworthy that vascularization was observed after extended culture times, but was not the primary objective of the study.

Metastasis is another hallmark of cancer, which consists of the sequential processes of cancer cell intravasation from the primary tumor into the vessels, migration through the vasculature, and extravasation into the secondary sites.<sup>5,6</sup> Tumor intravasation is influenced by multiple factors, including chemotactic gradients, oxygen levels, and impaired endothelial barriers.<sup>249</sup> For example, the transmigration of aggressive breast cancer cells (MDA-MB-231 cell line) across the endothelial layer has been observed under normal conditions, and was further enhanced after TNF- $\alpha$  treatment.<sup>242</sup> Similarly, Zervantonakis *et al.* explored the role of macrophages in intravasation, finding that macrophage-secreted TNF- $\alpha$  increases endothelial permeability, thereby enhancing the intravasation of fibrosarcoma cells<sup>250</sup> (Fig. 5B). Extravasation has been widely studied in both

2D<sup>251,252</sup> and 3D formats.<sup>253</sup> Jeon *et al.* modeled the organ-specific metastasis of breast cancer cells into a bone-like environment.<sup>253</sup> Several studies have focused on identifying parameters that facilitate extravasation. For example, a study shows that tumor cells physically trapped within blood vessels exhibit higher trans-endothelial migration efficiency compared to non-trapped cells, with similar findings for cell clusters *versus* individual tumor cells<sup>254</sup> (Fig. 5C). Another study demonstrated that hypoxic conditions increase extravasation, as shown using three different breast cancer cell lines.<sup>255</sup>

However, as both intravasation and extravasation predominantly occur in capillary-scale vessels, physiologically relevant vascular networks are required to obtain improved metastasis models. To accurately mimic both the tumor site and metastatic niche, vascular MPS should reflect not only capillary dimensions but also organ-specific endothelial characteristics. Indeed, Miles *et al.* discussed two complementary mechanisms of extravasation: the trapping model, where cells become physically trapped in capillaries, and the adhesion model, where tumor cells bind to specific endothelial markers in larger vessels.<sup>256–258</sup> Their findings underscore the critical roles of both vessel diameter and endothelial phenotype in regulating tumor cell arrest and transmigration. While a HUVEC-based model has successfully recapitulated tumor cell trapping *on-chip*,<sup>254</sup> 3D organ-specific microvascular models are required to investigate the relative contributions of adhesion *versus* trapping across different tumor types and metastatic niches. This limitation further highlights the previously discussed gap in self-organizing vascular MPS using organ-specific microvascular ECs and underscores the need for future studies to develop and apply such models for metastasis research.

**Immunity: immune responses and therapy.** Vascular MPS has also been used to model immune responses, as blood vessels are not only responsible for oxygen or nutrient delivery but also for transporting circulating cells such as platelets and immune cells. In the context of immunity, platelets are primarily associated with coagulation following vascular injury. While many studies have focused on platelet aggregation in the setting of thrombosis, hemostasis-on-chip models have also been developed to investigate bleeding responses.<sup>259</sup> These models replicate bleeding events using different methods, such as valve actuation to mimic a wound opening<sup>260</sup> or by needle puncture to mimic injuries,<sup>261</sup> both of which induce hemostasis. Additionally, the role of macrophages in coagulation has been explored using vascular MPS, further highlighting the complex interplay between immune cells and hemostatic processes.<sup>36</sup>

Beyond platelets, immune cells such as neutrophils, monocytes, dendritic cells, NK cells, and T cells play critical roles in immune surveillance and pathogen elimination. Neutrophils, as part of the innate immune system, serve as the first line of defense by targeting circulating pathogens within the vasculature through mechanisms such as

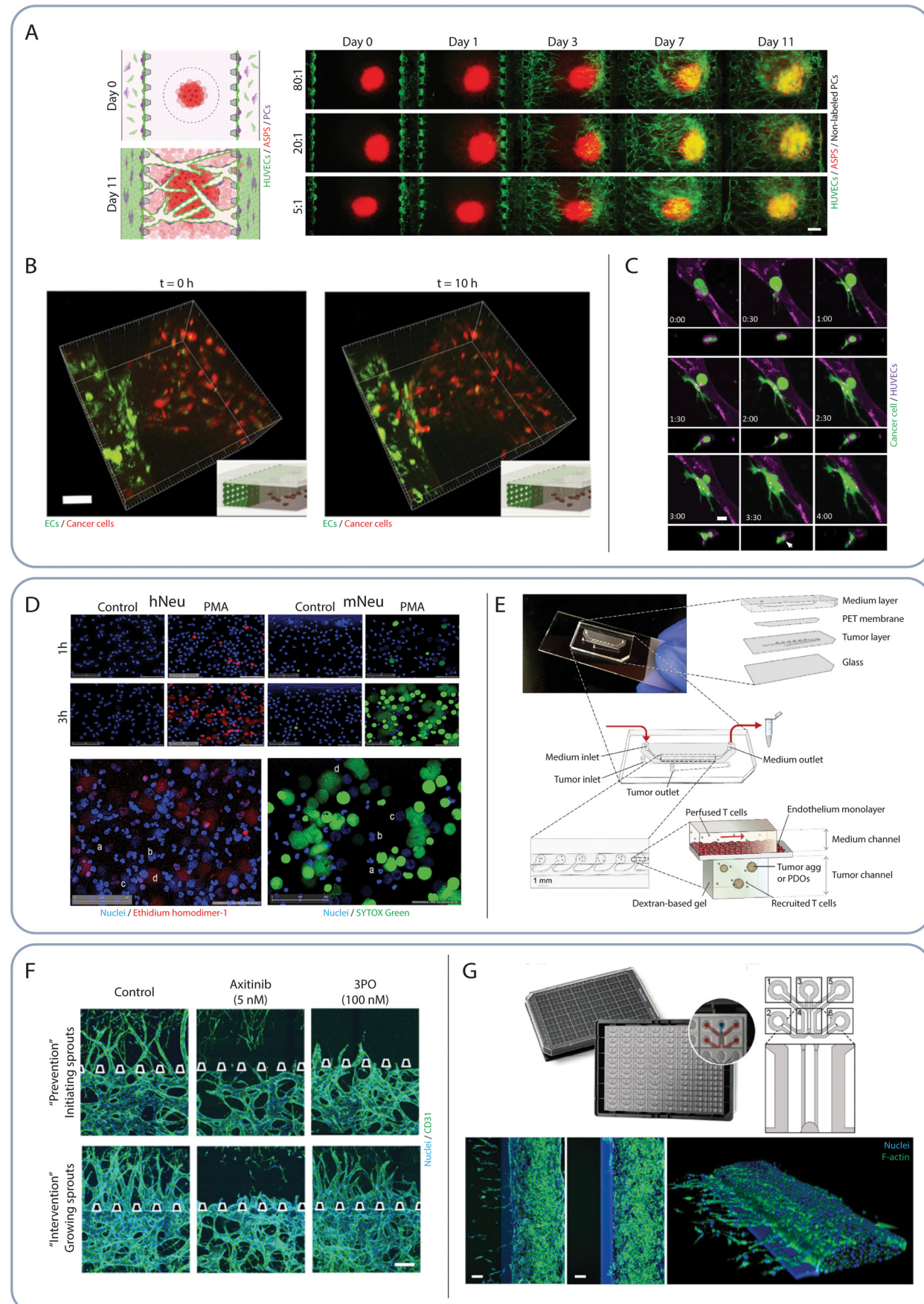


**Fig. 5** Vascular MPS for cancer recapitulation, immunity modeling, and drug screening. A) Alveolar soft part sarcoma (ASPS) model *on-chip*, using an angiogenesis method to vascularize the tumor spheroid.<sup>246</sup> Scale bar: 200  $\mu$ m. B) Intravasation of fibrosarcoma tumor cells (HT1080, red) from the ECM through the HUVEC monolayer (green) at 0 h and 10 h.<sup>250</sup> Inset shows image orientation in the device. Scale bar: 50  $\mu$ m. C) Extravasation of a tumor cell (MDA-MB-231, green) from the endothelium (purple).<sup>254</sup> Scale bar: 10  $\mu$ m. D) NET formation *on-chip* from human (hNeu) and monkey (mNeu) neutrophils, activated by 100 nM phorbol 12-myristate 13-acetate (PMA). Green is SYTOX-green, and red is ethidium homodimer-1, revealing DNA's presence. Letters a to d highlight different stages of NET formation.<sup>262</sup> The figure has been rearranged from the original. E) Device setup for immunotherapy *on-chip* using CAR-T cells targeting breast tumor cells, contained either in tumor aggregate or patient-derived organoids.<sup>271</sup> F) Drug assay, using 5 nM axitinib or 100  $\mu$ M 3PO, against angiogenic sprouts.<sup>57</sup> Either prevention or intervention methods have been applied, where drugs are injected before or during sprout formation, respectively. Scale bar: 200  $\mu$ m. The figure has been rearranged from the original. G) A high-throughput device used to perform angiogenesis phenotypic screening in response to various types of drugs.<sup>281</sup> Scale bars: 100  $\mu$ m. The figure has been rearranged from the original. All figures have been edited to enhance readability.

neutrophil extracellular traps (NETs). Yadav *et al.* demonstrated the utility of MPS for studying NET formation using pig ECs and blood<sup>262</sup> (Fig. 5D). Once pathogens are detected in tissues, immune cells extravasate from blood vessels into infected regions. MPS have replicated these processes, including monocyte extravasation,<sup>263</sup> dendritic cell migration,<sup>264</sup> and natural killer (NK) cell activity.<sup>265,266</sup> Ayuso *et al.* modeled NK cell targeting of solid tumors, supported by circulating antibodies,<sup>265</sup> while Humayun *et al.* targeted *Toxoplasma gondii*-infected cells.<sup>266</sup> Similarly, T cells' adhesion, crawling, and extravasation have been observed in a 3D vascular network.<sup>70</sup>

Immunity-on-chip has become of major interest in the MPS field, with efforts focused on developing both lymph node-on-chip models and integrated *on-chip* vascular-lymphatic networks. Analogous to angiogenesis, the role of flow has been demonstrated to enhance lymphatic vessel sprouting.<sup>267</sup> Additionally, lymphatic endothelial tubules have been used to explore the effect of shear stress, further advancing our understanding of lymphatic biology.<sup>268</sup> While standalone lymphatic vessel and lymph node *on-chip* models are still under development, the intrinsic relationship between blood and lymphatic vessels suggests that next-generation MPS will likely combine these two networks.<sup>269,270</sup> Such integrated systems could provide more comprehensive investigations of immune dynamics, including cell trafficking, antigen presentation, and systemic immune regulation.

From a biomedical and translational perspective, vascular MPS are increasingly employed in immunotherapy research, particularly in the evaluation of chimeric antigen receptor (CAR)-T cell therapies. For instance, Maulana *et al.* reported an *on-chip* breast cancer model to assess the efficacy of CAR-T cells in endothelial transmigration, tumor infiltration, and immune activation<sup>271</sup> (Fig. 5E). Similarly, CAR-T cells have been used in a vascularized *on-chip* model of ovarian tumor spheroids, derived from the Skov3 cell line.<sup>272</sup> This study shows that the spatial organization of the spheroid and, ultimately, the tumor architecture significantly impact therapeutic efficiency. Spheroids surrounded by fibroblasts exhibited higher vascularization and perfusability, compared to those with fibroblasts embedded within, which ultimately allowed an enhanced CAR-T cell delivery and more effective therapeutic assessment. Other models have also been designed to study CAR T-cell responses in ovarian and liver cancer models.<sup>273,274</sup>

**Drug screening: low and high throughput.** Given the critical role of vasculature in delivering drugs to target tissues, vascular MPS emerged as a powerful tool for drug-related studies. Additionally, the enactment of the Food and Drug Administration (FDA) Modernization Act 2.0 has further encouraged the use of non-animal models, opening new opportunities for MPS in drug testing and screening.<sup>275</sup> When considering *in vitro* platforms for drug evaluation, two parameters must be balanced: complexity and throughput. Complexity refers to how closely a model replicates the structure and function of real human tissues, while throughput refers to the number of samples that can be processed in a single experimental run. These parameters are often inversely related: highly complex models typically support low-throughput, whereas high-throughput platforms require simplification to maintain scalability. The appropriate balance depends on the research objective: low-throughput, high-complexity models are commonly used in academic settings for mechanistic studies, while high-throughput, lower-complexity models are favored in industry for efficient drug screening.

Low-throughput vascular MPS, while more intricate, are ideally suited for detailed analyses of drug delivery, efficacy, and mechanisms of action. These models typically assess one or a few compounds at a time, offering fine-grained insights into how drugs interact with tissue barriers and vasculature. For example, Kim *et al.* demonstrated that vascularizing lung tumor spheroid-on-chip enhanced both drug delivery and immune cell infiltration.<sup>276</sup> Using 2D devices, some studies assessed the transport of nanocarriers across endothelial barriers, such as the BBB.<sup>51</sup>

Drug assays in low-throughput vascular MPS usually aim to disrupt vascular networks, especially in cancer research, to target tumor vasculature. Studies often focus on disrupting already-formed vessels<sup>48,277</sup> or inhibiting angiogenesis.<sup>57</sup> Kim *et al.* tested two anti-angiogenic drugs, axitinib and 3PO, showing that axitinib inhibits both initiation and elongation of vascular sprouts, while 3PO is effective only during the initiation phase<sup>57</sup> (Fig. 5F). Similarly, vascularized organoid-on-chip models have been employed in drug assays, although there is still room for improvement.<sup>278</sup> One such study developed colorectal and breast cancer tumor spheroids, with both surrounding and penetrating vascular structures, to evaluate various drugs such as laninifab and cabozantinib. This study highlights their effectiveness in disrupting pre-

existing vasculature.<sup>48</sup> In contrast, some drug assays aim to enhance vasculature or restore functionality when vascular dysfunctions occur. For example, brain arteriovenous malformation, causing impaired vascular functionality, has been modeled using a vascular MPS and used for drug screening purposes.<sup>236</sup>

While traditional vascular MPS offer high functionality and relevance for drug testing, their inherently low throughput poses a major barrier to large-scale pharmaceutical screening. Addressing these challenges will be crucial for the broader adoption of MPS in industry. Towards that aim, multiplex systems have been developed to enable high-throughput microfluidic devices for vascular applications. These systems aim to balance physiological fidelity with scalability.<sup>37,279</sup> A first possible application is to perform vascular phenotypic screening, focusing on parameters such as angiogenic sprout morphology<sup>280</sup> and angiogenesis dynamics<sup>281</sup> (Fig. 5G). Secondly, disease-specific drug screening can be performed to determine potential treatments. Phan *et al.* developed a platform consisting of multiple vascularized micro-organs in a 96-well format, allowing for blind screening of a compound library, including anti-cancer drugs.<sup>279</sup> Wevers *et al.* demonstrated the application of a 384-well high-throughput BBB model, integrating 40 or 96 microfluidic chips for parallel screening.<sup>37</sup> Similar approaches have also been applied to study drug responses in fibrotic conditions<sup>282</sup> and aortic aneurysm.<sup>283</sup>

## Conclusion

Vascular MPS encompass diverse designs, ranging from 2D bilayer devices replicating endothelial–epithelial interfaces to 3D pre-patterned devices reconstructing vascular architecture, and self-organizing platforms which form *in vivo*-like networks through biological processes such as vasculogenesis and angiogenesis. While PDMS-based vascular MPS have proven highly effective in recapitulating vascular architecture, some limitations remain, particularly in modeling the wide range of vessel size and geometry. At the micro-scale, fabrication constraints restrict pre-patterned models, whereas self-organizing networks often yield vessels with diameters significantly larger than native capillaries. Typically less than 10 µm *in vivo*, *in vitro* vessels commonly range from 20 to 80 µm or more, especially in perfusable networks. As discussed previously, organ-specific microvascular ECs represent a promising approach to achieving capillary-scale modeling under both physiological and pathological conditions. For larger-scale vessels, PDMS-based fabrication relying on soft lithography is limited to rectangular, micrometer-scaled, and linear vessels. In contrast, native blood vessels range from micrometric to millimetric dimensions, with circular cross-sections and complex topologies. To address these limitations, 3D printing technologies have demonstrated significant potential in fabricating anatomically relevant vascular MPS.<sup>20–25</sup>

Blood vessels are complex structures composed of multiple cell types and are surrounded by a specific microenvironment. Capturing such complexity remains a common challenge for *in vitro* models. However, vascular MPS are steadily advancing in biological relevance. The first major improvement lies in cell sourcing. Vascular MPS now utilize more relevant cell types, such as organ-specific ECs or progenitor cells, shifting away from the conventional HUVECs toward more *in vivo*-like endothelium. The second advancement is the incorporation of perivascular cells, such as fibroblasts, pericytes, and SMCs. These additions enhance the stability and functionality of vascular MPS, both in healthy and diseased models. Recent years have also seen a growing interest in including other cell types, such as astrocytes, neurons, immune cells, and blood cells. The third improvement involves the use of *in vivo*-like acellular components. Membrane designs have evolved towards thinner membranes approximating basement membrane dimensions and electrospun membranes mimicking *in vivo* fibrillar organization. Additionally, ECM materials have transitioned from traditional hydrogels to more complex components, including dECM and synthetic polymers. Overall, as new sources and technologies for both cellular and acellular components continue to emerge, vascular MPS are poised to achieve greater biological relevance.

Current vascular MPS have demonstrated substantial capabilities for studying a broad range of vascular biology. Physical factors play a critical role in vascular biology, influencing blood vessel formation, stability, and functionality. For instance, intraluminal flow and resulting shear stress are key regulators of vascular organization and integrity, while interstitial flow has been strongly linked to the regulation of angiogenesis. Other mechanical factors, such as pressure and stretch, have also been recapitulated in vascular MPS, though they remain relatively understudied. An essential functionality of the endothelium is permeability, which varies depending on the organ and EC type.

Despite the current implementation of physical cues in vascular MPS, significant limitations persist for two main reasons: the lack of comprehensive theoretical values and the difficulty in experimental setups. Knowledge of *in vivo* values and physiological phenomena is still limited. For example, shear stress or permeability values are often derived from *in silico* simulations rather than empirical measurements, and data on interstitial flow, intraluminal pressure, and stretch are scarce in the literature. To address these gaps, theoretical advancements are necessary and should be thereafter integrated into vascular MPS studies. Simultaneously, experimental setups required to simulate these physical cues are often complex or labor-intensive. Developing more user-friendly or ready-to-use systems will be critical to enabling the routine incorporation of such physical factors into vascular MPS models.

In addition to studies on physical parameters, vascular MPS have enabled extensive exploration of biological aspects of vascular systems. These models have evolved from 2D co-

culture systems to more advanced 3D platforms, integrating vasculature with spheroids and organoids. In the context of tumor models, a vascular bed surrounding the spheroid is already a critical tool for studying the tumor microenvironment, vascular remodeling, and phenotypic changes in the endothelium. Yet, the need for intra-spheroid vascularization remains critical, as tumoral vasculature often presents distinct biological profiles and functional behaviors,<sup>284</sup> directly influencing drug delivery and therapeutic efficiency.<sup>284</sup> In organoids, the lack of perfusable vasculature leads to the formation of necrotic cores, as diffusion alone is insufficient to deliver nutrients to the center. Intra-organoid vascularization is thus essential for supporting further growth, preventing necrosis, and enabling the formation of more complex and mature structures. Overall, while integrating vasculature within organoids *on-chip* remains a significant challenge, progress in the next-generation organoids and vascular MPS is expected to make this integration increasingly feasible.

Finally, beyond physiological and organ-specific modeling, vascular MPS provide a robust platform for studying pathological conditions and developing clinical applications. These models have successfully modeled a wide range of vascular disorders *in vitro*, including thrombosis, hypertension, atherosclerosis, genetic vascular diseases, and infections. Their role in biomedical applications has further expanded to include immune response studies and drug testing. This translational relevance has been validated by the U.S. FDA's recognition of MPS for use in clinical development under the FDA Modernization Act 2.0, which allows MPS to serve as an alternative to animal models in defined contexts.<sup>275</sup> A remaining limitation, however, is throughput, particularly for PDMS-based MPS, which, despite offering higher throughput than animal models, still lag behind compared to 2D dish culture models. Encouragingly, recent developments in both academic and commercial MPS platforms, incorporating PDMS and alternative materials, have demonstrated promising improvements in throughput. While these innovations open doors for both vascular research and high-content drug screening, ongoing improvements in scalability and integration need to be sustained to fully establish vascular MPS as a standard tool in clinical and pharmaceutical research.

Overall, vascular MPS are highly valuable tools for studying a wide range of vascular-related physiological and pathological processes. Despite their current limitations, ongoing advancement in fabrication techniques, cell sourcing, acellular environment engineering, and technological innovation are poised to establish vascular MPS as a gold standard for vascular research.

## Data availability

No primary research results, software or code have been included and no new data were generated or analyzed as part of this review.

## Author contributions

Conceptualization: L. B., A. K., Y. S., H. Z., K. F., and R. Y. conceptualized the study. Funding acquisition: K. F. and R. Y. acquired the funding. Project administration: L. B. and R. Y. managed the project. Supervision: L. B. supervised the project. Visualization: L. B. designed the figures. Writing – original draft: L. B., A. K., Y. S., H. Z., and K. F. wrote the original draft. Writing – review & editing: L. B., A. K., Y. S., H. Z., K. F., and R. Y. reviewed and edited the manuscript.

## Conflicts of interest

All authors have agreed upon the publication of this manuscript. R. Y. is one of the founders and shareholders of Physios Biotech, Inc.

## Acknowledgements

This study was partially supported by the Japan Agency for Medical Research and Development: AMED-MPS (JP22be1004204 and JP17be0304205), AMEDP-PROMOTE (JP22ama221206), AMED P-CREATE (JP20cm0106277), and AMED-CREST (21gm1610005). The study was also supported by the Japan Society for the Promotion of Science: KAKENHI (JP24H00404, Grant-in-Aid for Scientific Research (A)), and KAKENHI (24K23941, International Leading Research: Creating a kidney). Finally, the study was supported by the "Advanced Research Infrastructure for Materials and Nanotechnology in Japan (ARIM)" of the Ministry of Education, Culture, Sports, Science and Technology (MEXT, JPMX1222KT1172). Illustrations were created with <https://Biorender.com>.

## References

- 1 S. S. Martin, A. W. Aday, Z. I. Almarzooq, C. A. M. Anderson, P. Arora and C. L. Avery, *et al.*, 2024 Heart Disease and Stroke Statistics: A Report of US and Global Data From the American Heart Association, *Circulation*, 2024, **149**(8), e347–e913.
- 2 More than 700 million people with untreated hypertension [Internet] [cited 2024 Nov 15], Available from: <https://www.who.int/news/item/25-08-2021-more-than-700-million-people-with-untreated-hypertension>.
- 3 A. M. D. Sheikh, S. Yano, S. Tabassum and A. Nagai, The Role of the Vascular System in Degenerative Diseases: Mechanisms and Implications, *Int. J. Mol. Sci.*, 2024, **25**(4), 2169.
- 4 R. A. Wimmer, A. Leopoldi, M. Aichinger, N. Wick, B. Hantusch and M. Novatchkova, *et al.*, Human blood vessel organoids as a model of diabetic vasculopathy, *Nature*, 2019, **565**(7740), 505–510.
- 5 D. Hanahan and R. A. Weinberg, The Hallmarks of Cancer, *Cell*, 2000, **100**(1), 57–70.
- 6 D. Hanahan and R. A. Weinberg, Hallmarks of Cancer: The Next Generation, *Cell*, 2011, **144**(5), 646–674.

7 M. Kapałczyńska, T. Kolenda, W. Przybyła, M. Zajączkowska, A. Teresiak and V. Filas, *et al.*, 2D and 3D cell cultures – a comparison of different types of cancer cell cultures, *Arch. Med. Sci.*, 2018, **14**(4), 910–919.

8 C. Jensen and Y. Teng, Is It Time to Start Transitioning From 2D to 3D Cell Culture?, *Front. Mol. Biosci.*, 2020, **7**, 33.

9 N. T. Doncheva, O. Palasca, R. Yarani, T. Litman, C. Anthon and M. A. M. Groenen, *et al.*, Human pathways in animal models: possibilities and limitations, *Nucleic Acids Res.*, 2021, **49**(4), 1859–1871.

10 T. Hartung, Thoughts on limitations of animal models, *Parkinsonism Relat. Disord.*, 2008, **14**, S81–S83.

11 M. J. Bledsoe and W. E. Grizzle, Use of human specimens in research: the evolving United States regulatory, policy, and scientific landscape, *Diagn. Histopathol.*, 2013, **19**(9), 322–330.

12 A. M. Taylor and B. Bordoni, Histology, Blood Vascular System, in *StatPearls [Internet]*, StatPearls Publishing, Treasure Island (FL), 2024, [cited 2024 Dec 11], Available from: <http://www.ncbi.nlm.nih.gov/books/NBK553217/>.

13 H. Mozafari, C. Zhou and L. Gu, Mechanical contribution of vascular smooth muscle cells in the tunica media of artery, *Nanotechnol. Rev.*, 2019, **8**(1), 50–60.

14 E. A. Tansey, L. E. A. Montgomery, J. G. Quinn, S. M. Roe and C. D. Johnson, Understanding basic vein physiology and venous blood pressure through simple physical assessments, *Adv. Physiol. Educ.*, 2019, **43**(3), 423–429.

15 M. W. Majesky and M. C. M. Weiser-Evans, The adventitia in arterial development, remodeling, and hypertension, *Biochem. Pharmacol.*, 2022, **205**, 115259.

16 T. Y. Tu and P. C.-P. Chao, Continuous blood pressure measurement based on a neural network scheme applied with a cuffless sensor, *Microsyst. Technol.*, 2018, **24**(11), 4539–4549.

17 D. Manning, E. J. Rivera and L. F. Santana, The life cycle of a capillary: Mechanisms of angiogenesis and rarefaction in microvascular physiology and pathologies, *Vasc. Pharmacol.*, 2024, **156**, 107393.

18 J. D. Kelley, C. C. Kerndt and J. V. Ashurst, Anatomy, Thorax, Aortic Arch, in *StatPearls [Internet]*, StatPearls Publishing, Treasure Island (FL), 2025, [cited 2025 May 1], Available from: <http://www.ncbi.nlm.nih.gov/books/NBK499911/>.

19 E. Bazigou and T. Makinen, Flow control in our vessels: vascular valves make sure there is no way back, *Cell. Mol. Life Sci.*, 2013, **70**(6), 1055–1066.

20 I. S. Kinstlinger and J. S. Miller, 3D-printed fluidic networks as vasculature for engineered tissue, *Lab Chip*, 2016, **16**(11), 2025–2043.

21 I. Matai, G. Kaur, A. Seyedsalehi, A. McClinton and C. T. Laurencin, Progress in 3D bioprinting technology for tissue/organ regenerative engineering, *Biomaterials*, 2020, **226**, 119536.

22 L. De Silva, P. N. Bernal, A. Rosenberg, J. Malda, R. Levato and D. Gawlitza, Biofabricating the vascular tree in engineered bone tissue, *Acta Biomater.*, 2023, **156**, 250–268.

23 Y. C. Hou, X. Cui, Z. Qin, C. Su, G. Zhang and J. N. Tang, *et al.*, Three-dimensional bioprinting of artificial blood vessel: Process, bioinks, and challenges, *Int. J. Bioprint.*, 2023, **9**(4), 740.

24 S. Li, H. Li, X. Shang, J. He and Y. Hu, Recent advances in 3D printing sacrificial templates for fabricating engineered vasculature, *MedComm: Biomater. Appl.*, 2023, **2**(3), e46.

25 X. Wu, W. Shi, X. Liu and Z. Gu, Recent advances in 3D-printing-based organ-on-a-chip, *EngMedicine*, 2024, **1**(1), 100003.

26 D. Huh, B. D. Matthews, A. Mammoto, M. Montoya-Zavala, H. Y. Hsin and D. E. Ingber, Reconstituting Organ-Level Lung Functions on a Chip, *Science*, 2010, **328**(5986), 1662–1668.

27 D. Qin, Y. Xia and G. M. Whitesides, Soft lithography for micro- and nanoscale patterning, *Nat. Protoc.*, 2010, **5**(3), 491–502.

28 I. Miranda, A. Souza, P. Sousa, J. Ribeiro, E. M. S. Castanheira and R. Lima, *et al.*, Properties and Applications of PDMS for Biomedical Engineering: A Review, *J. Funct. Biomater.*, 2021, **13**(1), 2.

29 S. Yadav, K. Fujimoto, T. Takenaga, S. Takahashi, Y. Muramoto and R. Mikawa, *et al.*, Isogenic iPSC-derived proximal and distal lung-on-chip models: Tissue- and virus-specific immune responses in human lungs, *bioRxiv*, 2023, preprint, DOI: [10.1101/2023.11.24.568532](https://doi.org/10.1101/2023.11.24.568532).

30 M. Zhang, P. Wang, R. Luo, Y. Wang, Z. Li and Y. Guo, *et al.*, Biomimetic Human Disease Model of SARS-CoV-2-Induced Lung Injury and Immune Responses on Organ Chip System, *Adv. Sci.*, 2021, **8**(3), 2002928.

31 A. J. Ainscough, T. J. Smith, M. Haensel, C. J. Rhodes, A. Fellows and H. J. Whitwell, *et al.*, An organ-on-chip model of pulmonary arterial hypertension identifies a BMPR2-SOX17-prostacyclin signalling axis, *Commun. Biol.*, 2022, **5**(1), 1192.

32 B. M. Maoz, A. Herland, E. A. Fitzgerald, T. Grevesse, C. Vidoudez and A. R. Pacheco, *et al.*, A linked organ-on-chip model of the human neurovascular unit reveals the metabolic coupling of endothelial and neuronal cells, *Nat. Biotechnol.*, 2018, **36**(9), 865–874.

33 K. Gold, A. K. Gaharwar and A. Jain, Emerging trends in multiscale modeling of vascular pathophysiology: Organ-on-a-chip and 3D Printing, *Biomaterials*, 2019, **196**, 2–17.

34 T. Y. Tu, Y. P. Shen, S. H. Lim and Y. K. Wang, A Facile Method for Generating a Smooth and Tubular Vessel Lumen Using a Viscous Fingering Pattern in a Microfluidic Device, *Front. Bioeng. Biotechnol.*, 2022, **10**, 877480.

35 S. W. Chen, A. Blazske, S. Zhang, S. E. Shelton, G. S. Offeddu and R. D. Kamm, Development of a perfusable, hierarchical microvasculature-on-a-chip model, *Lab Chip*, 2023, **23**(20), 4552–4564.

36 H. H. T. Middelkamp, H. J. Weener, T. Gensheimer, K. Vermeul, L. E. de Heus and H. J. Albers, *et al.*, Embedded macrophages induce intravascular coagulation in 3D blood vessel-on-chip, *Biomed. Microdevices*, 2024, **26**(1), 2.

37 N. R. Wevers, D. G. Kasi, T. Gray, K. J. Wilschut, B. Smith and R. Van Vugt, *et al.*, A perfused human blood–brain barrier on-a-chip for high-throughput assessment of barrier function and antibody transport, *Fluids Barriers CNS*, 2018, **15**(1), 23.

38 S. Fengler, B. Kurkowsky, S. K. Kaushalya, W. Roth, E. Fava and P. Denner, Human iPSC-derived brain endothelial microvessels in a multi-well format enable permeability screens of anti-inflammatory drugs, *Biomaterials*, 2022, **286**, 121525.

39 Y. Li, Y. Li, J. Li and H. Chen, Wall shear gradient dependent thrombosis studied in blood-on-a-chip with stenotic, branched, and valvular constructions, *Biomicrofluidics*, 2023, **17**(3), 034101.

40 N. K. R. Pandian, R. G. Mannino, W. A. Lam and A. Jain, Thrombosis-on-a-chip: Prospective impact of microphysiological models of vascular thrombosis, *Curr. Opin. Biomed. Eng.*, 2017, **5**, 29.

41 M. Lehmann, R. M. Schoeman, P. J. Krohl, A. M. Wallbank, J. R. Samaniuk and M. Jandrot-Perrus, *et al.*, Platelets Drive Thrombus Propagation in a Hematocrit and Glycoprotein VI-Dependent Manner in an In Vitro Venous Thrombosis Model, *Arterioscler., Thromb., Vasc. Biol.*, 2018, **38**(5), 1052–1062.

42 X. Hu, Y. Li, J. Li and H. Chen, Effects of altered blood flow induced by the muscle pump on thrombosis in a microfluidic venous valve model, *Lab Chip*, 2020, **20**(14), 2473–2481.

43 H. Dai, S. Chai, Y. Yao, W. Tang, J. Shi and Q. Jiang, *et al.*, Effect of intermittent pneumatic compression on preventing deep vein thrombosis using microfluidic vein chip, *Front. Bioeng. Biotechnol.*, 2023, **11**, 1281503.

44 Y. Li, Y. Li and H. Chen, The effect of ultrasound-assisted thrombolysis studied in blood-on-a-chip, *Artif. Organs*, 2024, **48**(7), 734–742.

45 M. Ibrahim and M. K. Richardson, Beyond organoids: In vitro vasculogenesis and angiogenesis using cells from mammals and zebrafish, *Reprod. Toxicol.*, 2017, **73**, 292–311.

46 O. V. Poveshchenko, A. F. Poveshchenko and V. I. Konenkov, Endothelial progenitor cells and neovasculogenesis, *Biol. Bull. Rev.*, 2012, **2**(4), 333–339.

47 M. L. Moya, Y. H. Hsu, A. P. Lee, C. C. W. Hughes and S. C. George, In Vitro Perfused Human Capillary Networks, *Tissue Eng., Part C*, 2013, **19**(9), 730–737.

48 A. Sobrino, D. T. T. Phan, R. Datta, X. Wang, S. J. Hachey and M. Romero-López, *et al.*, 3D microtumors in vitro supported by perfused vascular networks, *Sci. Rep.*, 2016, **6**(1), 31589.

49 Y. K. Kurokawa, R. T. Yin, M. R. Shang, V. S. Shirure, M. L. Moya and S. C. George, Human Induced Pluripotent Stem Cell-Derived Endothelial Cells for Three-Dimensional Microphysiological Systems, *Tissue Eng., Part C*, 2017, **23**(8), 474–484.

50 Y. Xiao, D. Kim, B. Dura, K. Zhang, R. Yan and H. Li, *et al.*, Ex vivo Dynamics of Human Glioblastoma Cells in a Microvasculature-on-a-Chip System Correlates with Tumor Heterogeneity and Subtypes, *Adv. Sci.*, 2019, **6**(8), 1801531.

51 S. W. L. Lee, M. Campisi, T. Osaki, L. Possenti, C. Mattu and G. Adriani, *et al.*, Modeling Nanocarrier Transport across a 3D In Vitro Human Blood-Brain-Barrier Microvasculature, *Adv. Healthcare Mater.*, 2020, **9**(7), 1901486.

52 V. V. Orlova, D. M. Nahon, A. Cochrane, X. Cao, C. Freund and F. van den Hil, *et al.*, Vascular defects associated with hereditary hemorrhagic telangiectasia revealed in patient-derived isogenic iPSCs in 3D vessels on chip, *Stem Cell Rep.*, 2022, **17**(7), 1536.

53 M. A. Winkelman, D. Y. Kim, S. Kakarla, A. Grath, N. Silvia and G. Dai, Interstitial flow enhances the formation, connectivity, and function of 3D brain microvascular networks generated within a microfluidic device, *Lab Chip*, 2021, **22**(1), 170–192.

54 S. Kim, H. Lee, M. Chung and N. L. Jeon, Engineering of functional, perfusable 3D microvascular networks on a chip, *Lab Chip*, 2013, **13**(8), 1489.

55 S. Oh, H. Ryu, D. Tahk, J. Ko, Y. Chung and H. K. Lee, *et al.*, “Open-top” microfluidic device for in vitro three-dimensional capillary beds, *Lab Chip*, 2017, **17**(20), 3405–3414.

56 K. Fujimoto, Y. Kameda, Y. Nagano, S. Deguchi, T. Yamamoto and R. P. Krol, *et al.*, SARS-CoV-2-induced disruption of a vascular bed in a microphysiological system caused by type-I interferon from bronchial organoids, *Lab Chip*, 2024, **24**(16), 3863–3879.

57 S. Kim, M. Chung, J. Ahn, S. Lee and N. L. Jeon, Interstitial flow regulates the angiogenic response and phenotype of endothelial cells in a 3D culture model, *Lab Chip*, 2016, **16**(21), 4189–4199.

58 V. Van Duinen, D. Zhu, C. Ramakers, A. J. Van Zonneveld, P. Vullo and T. Hankemeier, Perfused 3D angiogenic sprouting in a high-throughput in vitro platform, *Angiogenesis*, 2019, **22**(1), 157–165.

59 J. Kim, M. Chung, S. Kim, D. H. Jo, J. H. Kim, N. L. Jeon and J. W. Lee, Engineering of a Biomimetic Pericyte-Covered 3D Microvascular Network, *PLoS One*, 2015, **10**(7), e0133880.

60 M. Chung, J. Ahn, K. Son, S. Kim and N. L. Jeon, Biomimetic Model of Tumor Microenvironment on Microfluidic Platform, *Adv. Healthcare Mater.*, 2017, **6**(15), 1700196.

61 S. Balaji, A. King, T. M. Crombleholme and S. G. Keswani, The Role of Endothelial Progenitor Cells in Postnatal Vasculogenesis: Implications for Therapeutic Neovascularization and Wound Healing, *Adv. Wound Care*, 2013, **2**(6), 283–295.

62 J. A. Whisler, M. B. Chen and R. D. Kamm, Control of Perfusion Microvascular Network Morphology Using a Multiculture Microfluidic System, *Tissue Eng., Part C*, 2014, **20**(7), 543–552.

63 D. H. T. Nguyen, E. Lee, S. Alimperti, R. J. Norgard, A. Wong and J. J. K. Lee, *et al.*, A biomimetic pancreatic cancer on-chip reveals endothelial ablation via ALK7 signaling, *Sci. Adv.*, 2019, **5**(8), eaav6789.

64 R. B. Sadeghian, R. Ueno, Y. Takata, A. Kawakami, C. Ma and T. Araoka, *et al.*, Cells sorted off hiPSC-derived kidney organoids coupled with immortalized cells reliably model the proximal tubule, *Commun. Biol.*, 2023, **6**(1), 483.

65 Y. Nashimoto, T. Hayashi, I. Kunita, A. Nakamasu, Y. S. Torisawa and M. Nakayama, *et al.*, Integrating perfusable vascular networks with a three-dimensional tissue in a microfluidic device, *Integr. Biol.*, 2017, **9**(6), 506–518.

66 H. Lee, S. Kim, M. Chung, J. H. Kim and N. L. Jeon, A bioengineered array of 3D microvessels for vascular permeability assay, *Microvasc. Res.*, 2014, **91**, 90–98.

67 R. Cao, Y. Wang, J. Liu, L. Rong and J. Qin, Self-assembled human placental model from trophoblast stem cells in a dynamic organ-on-a-chip system, *Cell Proliferation*, 2023, **56**(5), e13469.

68 K. Haase, M. R. Gillrie, C. Hajal and R. D. Kamm, Pericytes Contribute to Dysfunction in a Human 3D Model of Placental Microvasculature through VEGF-Ang-Tie2 Signaling, *Adv. Sci.*, 2019, **6**(23), 1900878.

69 Y. Nashimoto, R. Okada, S. Hanada, Y. Arima, K. Nishiyama and T. Miura, *et al.*, Vascularized cancer on a chip: The effect of perfusion on growth and drug delivery of tumor spheroid, *Biomaterials*, 2020, **229**, 119547.

70 E. Hirth, W. Cao, M. Peltonen, E. Kapetanovic, C. Dietsche and S. Svanberg, *et al.*, Self-assembled and perfusable microvasculature-on-chip for modeling leukocyte trafficking, *Lab Chip*, 2024, **24**(2), 292–304.

71 L. Prodanov, R. Jindal, S. S. Bale, M. Hegde, W. J. McCarty and I. Golberg, *et al.*, Long-term maintenance of a microfluidic 3D human liver sinusoid, *Biotechnol. Bioeng.*, 2016, **113**(1), 241–246.

72 N. Kumar, B. Samanta, J. Km, V. Raghunathan, P. Sen and R. Bhat, Demonstration of Enhancement of Tumor Intravasation by Dicarbonyl Stress Using a Microfluidic Organ-on-chip, *Small*, 2025, **21**(6), 2405998.

73 F. Vega-Tapia, E. Peñaloza and B. J. Krause, Specific arterio-venous transcriptomic and ncRNA-RNA interactions in human umbilical endothelial cells: A meta-analysis, *iScience*, 2021, **24**(6), 102675.

74 M. Potente and T. Mäkinen, Vascular heterogeneity and specialization in development and disease, *Nat. Rev. Mol. Cell Biol.*, 2017, **18**(8), 477–494.

75 E. Trimm and K. Red-Horse, Vascular endothelial cell development and diversity, *Nat. Rev. Cardiol.*, 2023, **20**(3), 197–210.

76 J. Kalucka, L. P. M. H. De Rooij, J. Goveia, K. Rohlenova, S. J. Dumas and E. Meta, *et al.*, Single-Cell Transcriptome Atlas of Murine Endothelial Cells, *Cell*, 2020, **180**(4), 764–779.e20.

77 O. Bondareva, J. R. Rodríguez-Aguilera, F. Oliveira, L. Liao, A. Rose and A. Gupta, *et al.*, Single-cell profiling of vascular endothelial cells reveals progressive organ-specific vulnerabilities during obesity, *Nat. Metab.*, 2022, **4**(11), 1591–1610.

78 V. V. Thacker, K. Sharma, N. Dhar, G. Mancini, J. Sordet-Dessimoz and J. D. McKinney, Rapid endotheliitis and vascular damage characterize SARS-CoV-2 infection in a human lung-on-chip model, *EMBO Rep.*, 2021, **22**(6), e52744.

79 L. Si, H. Bai, M. Rodas, W. Cao, C. Y. Oh and A. Jiang, *et al.*, A human-airway-on-a-chip for the rapid identification of candidate antiviral therapeutics and prophylactics, *Nat. Biomed. Eng.*, 2021, **5**(8), 815–829.

80 R. Hashimoto, J. Takahashi, K. Shirakura, R. Funatsu, K. Kosugi and S. Deguchi, *et al.*, SARS-CoV-2 disrupts respiratory vascular barriers by suppressing Claudin-5 expression, *Sci. Adv.*, 2022, **8**(38), eab06783.

81 N. Y. C. Lin, K. A. Homan, S. S. Robinson, D. B. Kolesky, N. Duarte and A. Moisan, *et al.*, Renal reabsorption in 3D vascularized proximal tubule models, *Proc. Natl. Acad. Sci. U. S. A.*, 2019, **116**(12), 5399–5404.

82 Y. Du, N. Li, H. Yang, C. Luo, Y. Gong and C. Tong, *et al.*, Mimicking liver sinusoidal structures and functions using a 3D-configured microfluidic chip, *Lab Chip*, 2017, **17**(5), 782–794.

83 M. Urbanczyk, A. Zbinden and K. Schenke-Layland, Organ-specific endothelial cell heterogeneity and its impact on regenerative medicine and biomedical engineering applications, *Adv. Drug Delivery Rev.*, 2022, **186**, 114323.

84 H. Uwamori, Y. Ono, T. Yamashita, K. Arai and R. Sudo, Comparison of organ-specific endothelial cells in terms of microvascular formation and endothelial barrier functions, *Microvasc. Res.*, 2019, **122**, 60–70.

85 M. R. Carvalho, D. Barata, L. M. Teixeira, S. Giselbrecht, R. L. Reis and J. M. Oliveira, *et al.*, Colorectal tumor-on-a-chip system: A 3D tool for precision onco-nanomedicine, *Sci. Adv.*, 2019, **5**(5), eaaw1317.

86 O. Jung, Y. T. Tung, E. Sim, Y. C. Chen, E. Lee and M. Ferrer, *et al.*, Development of human-derived, three-dimensional respiratory epithelial tissue constructs with perfusable microvasculature on a high-throughput microfluidics screening platform, *Biofabrication*, 2022, **14**(2), 025012.

87 S. J. Hachey, S. Movsesyan, Q. H. Nguyen, G. Burton-Sojo, A. Tankazyan and J. Wu, *et al.*, An in vitro vascularized micro-tumor model of human colorectal cancer recapitulates in vivo responses to standard-of-care therapy, *Lab Chip*, 2021, **21**(7), 1333–1351.

88 N. Kosyakova, D. D. Kao, M. Figetakis, F. López-Giráldez, S. Spindler and M. Graham, *et al.*, Differential functional roles of fibroblasts and pericytes in the formation of tissue-engineered microvascular networks in vitro, *npj Regener. Med.*, 2020, **5**(1), 1.

89 H. J. Joo, S. Song, H. R. Seo, J. H. Shin, S. C. Choi and J. H. Park, *et al.*, Human endothelial colony forming cells from adult peripheral blood have enhanced sprouting angiogenic potential through up-regulating VEGFR2 signaling, *Int. J. Cardiol.*, 2015, **197**, 33–43.

90 M. Virumbrales-Muñoz, J. M. Ayuso, J. R. Loken, K. M. Denecke, S. Rehman and M. C. Skala, *et al.*, Microphysiological model of renal cell carcinoma to inform anti-angiogenic therapy, *Biomaterials*, 2022, **283**, 121454.

91 S. Browne, E. L. Gill, P. Schultheiss, I. Goswami and K. E. Healy, Stem cell-based vascularization of microphysiological systems, *Stem Cell Rep.*, 2021, **16**(9), 2058–2075.

92 L. Perry, M. Y. Flugelman and S. Levenberg, Elderly Patient-Derived Endothelial Cells for Vascularization of Engineered Muscle, *Mol. Ther.*, 2017, **25**(4), 935–948.

93 C. C. Hughes, Endothelial-stromal interactions in angiogenesis, *Curr. Opin. Hematol.*, 2008, **15**(3), 204–209.

94 A. C. Newman, M. N. Nakatsu, W. Chou, P. D. Gershon and C. C. W. Hughes, The requirement for fibroblasts in angiogenesis: fibroblast-derived matrix proteins are essential for endothelial cell lumen formation, *Mol. Biol. Cell*, 2011, **22**(20), 3791–3800.

95 O. C. Velazquez, R. Snyder, Z. Liu, R. M. Fairman and M. Herlyn, Fibroblast-dependent differentiation of human microvascular endothelial cells into capillary-like, three-dimensional networks, *FASEB J.*, 2002, **16**(10), 1316–1318.

96 J. Whisler, S. Shahreza, K. Schlegelmilch, N. Ege, Y. Javanmardi and A. Malandrino, *et al.*, Emergent mechanical control of vascular morphogenesis, *Sci. Adv.*, 2023, **9**(32), eadg9781.

97 R. J. Luu, B. C. Hoefer, A. L. Gard, C. R. Ritenour, M. T. Rogers and E. S. Kim, *et al.*, Fibroblast activation in response to TGF $\beta$ 1 is modulated by co-culture with endothelial cells in a vascular organ-on-chip platform, *Front. Mol. Biosci.*, 2023, **10**, 1160851.

98 A. Holm, T. Heumann and H. G. Augustin, Microvascular Mural Cell Organotypic Heterogeneity and Functional Plasticity, *Trends Cell Biol.*, 2018, **28**(4), 302–316.

99 X. Zhang, M. Bishawi, G. Zhang, V. Prasad, E. Salmon and J. J. Breithaupt, *et al.*, Modeling early stage atherosclerosis in a primary human vascular microphysiological system, *Nat. Commun.*, 2020, **11**(1), 5426.

100 M. V. Cuenca, A. Cochrane, F. E. Van Den Hil, A. A. F. De Vries, S. A. J. L. Oberstein and C. L. Mummery, *et al.*, Engineered 3D vessel-on-chip using hiPSC-derived endothelial- and vascular smooth muscle cells, *Stem Cell Rep.*, 2021, **16**(9), 2159–2168.

101 L. Muhl, G. Genové, S. Leptidis, J. Liu, L. He and G. Mocci, *et al.*, Single-cell analysis uncovers fibroblast heterogeneity and criteria for fibroblast and mural cell identification and discrimination, *Nat. Commun.*, 2020, **11**(1), 3953.

102 M. Vanlandewijck, L. He, M. A. Mäe, J. Andrae, K. Ando and F. Del Gaudio, *et al.*, A molecular atlas of cell types and zonation in the brain vasculature, *Nature*, 2018, **554**(7693), 475–480.

103 V. L. Payen, A. Lavergne, N. A. Sarika, M. Colonval, L. Karim and M. Deckers, *et al.*, Single-cell RNA sequencing of human liver reveals hepatic stellate cell heterogeneity, *JHEP Rep.*, 2021, **3**(3), 100278.

104 A. R. England, C. P. Chaney, A. Das, M. Patel, A. Malewska and D. Armendariz, *et al.*, Identification and characterization of cellular heterogeneity within the developing renal interstitium, *Development*, 2020, dev.190108.

105 E. A. Margolis, D. S. Cleveland, Y. P. Kong, J. A. Beamish, W. Y. Wang and B. M. Baker, *et al.*, Stromal cell identity modulates vascular morphogenesis in a microvasculature-on-a-chip platform, *Lab Chip*, 2021, **21**(6), 1150–1163.

106 L. Wang, P. Dorn, S. Zeinali, L. Froment, S. Berezowska and G. J. Kocher, *et al.*, CD90 $^+$  CD146 $^+$  identifies a pulmonary mesenchymal cell subtype with both immune modulatory and perivascular-like function in postnatal human lung, *Am. J. Physiol.*, 2020, **318**(4), L813–L830.

107 G. D. Vatine, R. Barrile, M. J. Workman, S. Sances, B. K. Barriga and M. Rahnama, *et al.*, Human iPSC-Derived Blood-Brain Barrier Chips Enable Disease Modeling and Personalized Medicine Applications, *Cell Stem Cell*, 2019, **24**(6), 995–1005.e6.

108 K. Doi, H. Kimura, Y. T. Matsunaga, T. Fujii and M. Nangaku, Glomerulus-on-a-Chip: Current Insights and Future Potential Towards Recapitulating Selectively Permeable Filtration Systems, *Int. J. Nephrol. Renovasc. Dis.*, 2022, **15**, 85–101.

109 S. I. Ahn, Y. J. Sei, H. J. Park, J. Kim, Y. Ryu and J. J. Choi, *et al.*, Microengineered human blood-brain barrier platform for understanding nanoparticle transport mechanisms, *Nat. Commun.*, 2020, **11**(1), 175.

110 Y. Guo, R. Luo, Y. Wang, P. Deng, T. Song and M. Zhang, *et al.*, SARS-CoV-2 induced intestinal responses with a biomimetic human gut-on-chip, *Sci. Bull.*, 2021, **66**(8), 783–793.

111 M. Zhou, X. Zhang, X. Wen, T. Wu, W. Wang and M. Yang, *et al.*, Development of a Functional Glomerulus at the Organ Level on a Chip to Mimic Hypertensive Nephropathy, *Sci. Rep.*, 2016, **6**(1), 31771.

112 B. Mosavati, A. V. Oleinikov and E. Du, Development of an Organ-on-a-Chip-Device for Study of Placental Pathologies, *Int. J. Mol. Sci.*, 2020, **21**(22), 8755.

113 D. Hudecz, T. Khire, H. L. Chung, L. Adumeau, D. Glavin and E. Luke, *et al.*, Ultrathin Silicon Membranes for In Situ Optical Analysis of Nanoparticle Translocation Across a Human Blood-Brain Barrier Model, *ACS Nano*, 2020, **14**(1), 1111.

114 D. Hudecz, M. C. McCloskey, S. Vergo, S. Christensen, J. L. McGrath and M. S. Nielsen, Modelling a Human Blood-Brain Barrier Co-Culture Using an Ultrathin Silicon Nitride Membrane-Based Microfluidic Device, *Int. J. Mol. Sci.*, 2023, **24**(6), 5624.

115 A. K. Nicholas and P. B. Jacques, Morphology and Ultrastructure of Basement Membranes, in *Current Topics in Membranes*, Academic Press, 2005, vol. 56, p. 1942.

116 W. Halfter, P. Oertle, C. A. Monnier, L. Camenzind, M. Reyes-Lua and H. Hu, *et al.*, New concepts in basement membrane biology, *FEBS J.*, 2015, **282**(23), 4466–4479.

117 H. Li, Y. Zheng, Y. L. Han, S. Cai and M. Guo, Nonlinear elasticity of biological basement membrane revealed by rapid inflation and deflation, *Proc. Natl. Acad. Sci. U. S. A.*, 2021, **118**(11), e2022422118.

118 U. Töpfer, Basement membrane dynamics and mechanics in tissue morphogenesis, *Biol. Open*, 2023, **12**(8), bio059980.

119 J. Youn, H. Hong, W. Shin, D. Kim, H. J. Kim and D. S. Kim, Thin and stretchable extracellular matrix (ECM) membrane reinforced by nanofiber scaffolds for developing in vitro barrier models, *Biofabrication*, 2022, **14**(2), 025010.

120 J. Youn, H. Han, S. M. Park and D. S. Kim, Arterial Internal Elastic Lamina-Inspired Membrane for Providing Biochemical and Structural Cues in Developing Artery-on-a-Chip, *ACS Macro Lett.*, 2021, **10**(11), 1398–1403.

121 H. Moghadas, M. S. Saidi, N. Kashaninejad and N. T. Nguyen, A high-performance polydimethylsiloxane electrospun membrane for cell culture in lab-on-a-chip, *Biomicrofluidics*, 2018, **12**(2), 024117.

122 K. Man, J. Liu, C. Liang, C. Corona, M. D. Story and B. Meckes, *et al.*, Biomimetic Human Lung Alveolar Interstitium Chip with Extended Longevity, *ACS Appl. Mater. Interfaces*, 2023, **15**(30), 36888–36898.

123 P. Kanabekova, B. Dauletkanov, Z. Bekezhankzyzy, S. Toktarkan, A. Martin and T. T. Pham, *et al.*, A hybrid fluorescent nanofiber membrane integrated with microfluidic chips towards lung-on-a-chip applications, *Lab Chip*, 2024, **24**(2), 224–233.

124 W. Chen, F. Li, L. Chen, Y. Zhang, T. Zhang and T. Wang, Fast self-assembly of microporous silk fibroin membranes on liquid surface, *Int. J. Biol. Macromol.*, 2020, **156**, 633–639.

125 C. P. Tasiopoulos, L. Gustafsson, W. Van Der Wijngaart and M. Hedhammar, Fibrillar Nanomembranes of Recombinant Spider Silk Protein Support Cell Co-culture in an In Vitro Blood Vessel Wall Model, *ACS Biomater. Sci. Eng.*, 2021, **7**(7), 3332–3339.

126 M. Kitsara, P. Joanne, S. E. Boitard, I. B. Dhiab, B. Poinard and P. Menasché, *et al.*, Fabrication of cardiac patch by using electrospun collagen fibers, *Microelectron. Eng.*, 2015, **144**, 46–50.

127 M. Tahir, S. Vicini and A. Sionkowska, Electrospun Materials Based on Polymer and Biopolymer Blends—A Review, *Polymers*, 2023, **15**(7), 1654.

128 S. Bersini and M. Moretti, 3D functional and perfusable microvascular networks for organotypic microfluidic models, *J. Mater. Sci.: Mater. Med.*, 2015, **26**(5), 180.

129 D. Wang, T. Brady, L. Santhanam and S. Gerecht, The extracellular matrix mechanics in the vasculature, *Nat. Cardiovasc. Res.*, 2023, **2**(8), 718–732.

130 K. M. Noh, S. J. Park, S. H. Moon and S. Y. Jung, Extracellular matrix cues regulate the differentiation of pluripotent stem cell-derived endothelial cells, *Front. Cardiovasc. Med.*, 2023, **10**, 1169331.

131 C. Bonnans, J. Chou and Z. Werb, Remodelling the extracellular matrix in development and disease, *Nat. Rev. Mol. Cell Biol.*, 2014, **15**(12), 786–801.

132 J. Xu and G. P. Shi, Vascular wall extracellular matrix proteins and vascular diseases, *Biochim. Biophys. Acta, Mol. Basis Dis.*, 2014, **1842**(11), 2106–2119.

133 H. Trębacz and A. Barzycka, Mechanical Properties and Functions of Elastin: An Overview, *Biomolecules*, 2023, **13**(3), 574.

134 R. Hallmann, N. Horn, M. Selg, O. Wendler, F. Pausch and L. M. Sorokin, Expression and Function of Laminins in the Embryonic and Mature Vasculature, *Physiol. Rev.*, 2005, **85**(3), 979–1000.

135 S. Ghatak, E. V. Maytin, J. A. Mack, V. C. Hascall, I. Atanelishvili and R. M. Rodriguez, *et al.*, Roles of Proteoglycans and Glycosaminoglycans in Wound Healing and Fibrosis, *Int. J. Cell Biol.*, 2015, **2015**, 834893.

136 A. Barkovskaya, A. Buffone, M. Žídek and V. M. Weaver, Proteoglycans as Mediators of Cancer Tissue Mechanics, *Front. Cell Dev. Biol.*, 2020, **8**, 569377.

137 E. A. Lenselink, Role of fibronectin in normal wound healing, *Int. Wound J.*, 2013, **12**(3), 313–316.

138 J. Patten and K. Wang, Fibronectin in development and wound healing, *Adv. Drug Delivery Rev.*, 2021, **170**, 353–368.

139 A. J. Lepedda, G. Nieddu, M. Formato, M. B. Baker, J. Fernández-Pérez and L. Moroni, Glycosaminoglycans: From Vascular Physiology to Tissue Engineering Applications, *Front. Chem.*, 2021, **9**, 680836.

140 F. Bonanini, D. Kurek, S. Previdi, A. Nicolas, D. Hendriks and S. de Ruiter, *et al.*, In vitro grafting of hepatic spheroids and organoids on a microfluidic vascular bed, *Angiogenesis*, 2022, **25**, 455470.

141 J. W. Song and L. L. Munn, Fluid forces control endothelial sprouting, *Proc. Natl. Acad. Sci. U. S. A.*, 2011, **108**(37), 15342–15347.

142 K. Fujimoto, S. Erickson, M. Nakayama, H. Ihara, K. Sugihara and Y. Nashimoto, *et al.*, Pericytes and shear stress each alter the shape of a self-assembled vascular network, *Lab Chip*, 2023, **23**(2), 306–317.

143 J. H. Yeon, H. R. Ryu, M. Chung, Q. P. Hu and N. L. Jeon, In vitro formation and characterization of a perfusable three-dimensional tubular capillary network in microfluidic devices, *Lab Chip*, 2012, **12**(16), 2815–2822.

144 C. L. E. Helm, A. Zisch and M. A. Swartz, Engineered blood and lymphatic capillaries in 3-D VEGF-fibrin-collagen matrices with interstitial flow, *Biotechnol. Bioeng.*, 2007, **96**(1), 167–176.

145 M. B. Chen, S. Srigunapalan, A. R. Wheeler and C. A. Simmons, A 3D microfluidic platform incorporating methacrylated gelatin hydrogels to study physiological cardiovascular cell-cell interactions, *Lab Chip*, 2013, **13**(13), 2591.

146 H. Liu, M. Jie, Z. He, H. F. Li and J. M. Lin, Study of antioxidant effects on malignant glioma cells by constructing a tumor-microvascular structure on microchip, *Anal. Chim. Acta*, 2017, **978**, 1–9.

147 H. K. Kleinman and G. R. Martin, Matrigel: basement membrane matrix with biological activity, *Semin. Cancer Biol.*, 2005, **15**(5), 378–386.

148 L. Wang, T. Tao, W. Su, H. Yu, Y. Yu and J. Qin, A disease model of diabetic nephropathy in a glomerulus-on-a-chip microdevice, *Lab Chip*, 2017, **17**(10), 1749–1760.

149 M. Zhang, C. Xu, L. Jiang and J. Qin, A 3D human lung-on-a-chip model for nanotoxicity testing, *Toxicol. Res.*, 2018, **7**(6), 1048–1060.

150 F. Yin, Y. Zhu, M. Zhang, H. Yu, W. Chen and J. Qin, A 3D human placenta-on-a-chip model to probe nanoparticle exposure at the placental barrier, *Toxicol. In Vitro*, 2019, **54**, 105–113.

151 X. Zhang, X. Chen, H. Hong, R. Hu, J. Liu and C. Liu, Decellularized extracellular matrix scaffolds: Recent trends and emerging strategies in tissue engineering, *Bioact. Mater.*, 2021, **10**, 15–31.

152 E. V. Isaeva, E. E. Beketov, N. V. Arguchinskaya, S. A. Ivanov, P. V. Shegay and A. D. Kaprin, Decellularized Extracellular Matrix for Tissue Engineering (Review), *Sovrem. Tehnol. v Med.*, 2022, **14**(3), 57–68.

153 L. Zhu, J. Yuhan, H. Yu, B. Zhang, K. Huang and L. Zhu, Decellularized Extracellular Matrix for Remodeling Bioengineering Organoid's Microenvironment, *Small*, 2023, **19**(25), 2207752.

154 T. Hoshiba, Decellularized Extracellular Matrix for Cancer Research, *Materials*, 2019, **12**(8), 1311.

155 A. N. Cho, Y. Jin, Y. An, J. Kim, Y. S. Choi and J. S. Lee, *et al.*, Microfluidic device with brain extracellular matrix promotes structural and functional maturation of human brain organoids, *Nat. Commun.*, 2021, **12**(1), 4730.

156 J. W. Kim, S. A. Nam, J. Yi, J. Y. Kim, J. Y. Lee and S. Park, *et al.*, Kidney Decellularized Extracellular Matrix Enhanced the Vascularization and Maturation of Human Kidney Organoids, *Adv. Sci.*, 2022, **9**(15), 2103526.

157 M. F. B. Jamaluddin, A. Ghosh, A. Ingle, R. Mohammed, A. Ali and M. Bahrami, *et al.*, Bovine and human endometrium-derived hydrogels support organoid culture from healthy and cancerous tissues, *Proc. Natl. Acad. Sci. U. S. A.*, 2022, **119**(44), e2208040119.

158 Z. Wang, R. Liu, Y. Liu, Y. Zhao, Y. Wang and B. Lu, *et al.*, Human Placenta Decellularized Extracellular Matrix Hydrogel Promotes the Generation of Human Spinal Cord Organoids with Dorsorostral Organization from Human Induced Pluripotent Stem Cells, *ACS Biomater. Sci. Eng.*, 2024, **10**(5), 3218–3231.

159 W. Wu, Y. Liu, R. Liu, Y. Wang, Y. Zhao and H. Li, *et al.*, Decellularized Brain Extracellular Matrix Hydrogel Aids the Formation of Human Spinal-Cord Organoids Recapitulating the Complex Three-Dimensional Organization, *ACS Biomater. Sci. Eng.*, 2024, **10**(5), 3203–3217.

160 S. Lu, F. Cuzzucoli, J. Jiang, L. G. Liang, Y. Wang and M. Kong, *et al.*, Development of a biomimetic liver tumor-on-a-chip model based on decellularized liver matrix for toxicity testing, *Lab Chip*, 2018, **18**(22), 3379–3392.

161 A. Bhatt, N. Dhiman, P. S. Giri, G. N. Kasinathan, F. Pati and S. N. Rath, Biocompatibility-on-a-chip: Characterization and evaluation of decellularized tendon extracellular matrix (tdECM) hydrogel for 3D stem cell culture in a microfluidic device, *Int. J. Biol. Macromol.*, 2022, **213**, 768–779.

162 E. Fernandez-Carro, A. R. Remacha, I. Orera, G. Lattanzio, A. Garcia-Barrios and J. Del Barrio, *et al.*, Human Dermal Decellularized ECM Hydrogels as Scaffolds for 3D In Vitro Skin Aging Models, *Int. J. Mol. Sci.*, 2024, **25**(7), 4020.

163 Z. Lu, X. Miao, C. Zhang, B. Sun, A. Skardal and A. Atala, *et al.*, An osteosarcoma-on-a-chip model for studying osteosarcoma matrix-cell interactions and drug responses, *Bioact. Mater.*, 2024, **34**, 1–16.

164 W. Hu, H. P. Bei, H. Jiang, D. Wu, X. Yu and X. Zhou, *et al.*, DLM-GelMA/tumor slice sandwich structured tumor on a chip for drug efficacy testing, *Lab Chip*, 2024, **24**(15), 3718–3727.

165 T. Kollmetz, F. Castillo-Alcalá, R. W. F. Veale, N. Taghavi, V. M. van Heeswijk and M. Persenaire, *et al.*, Comparative Analysis of Commercially Available Extracellular Matrix Soft Tissue Bioscaffolds, *Tissue Eng., Part A*, 2024, **31**(11–12), 442–455.

166 E. H. Nguyen, W. T. Daly, N. N. T. Le, M. Farnoodian, D. G. Belair and M. P. Schwartz, *et al.*, Versatile synthetic alternatives to Matrigel for vascular toxicity screening and stem cell expansion, *Nat. Biomed. Eng.*, 2017, **1**, 0096.

167 M. P. Cuchiara, A. C. B. Allen, T. M. Chen, J. S. Miller and J. L. West, Multilayer microfluidic PEGDA hydrogels, *Biomaterials*, 2010, **31**(21), 5491–5497.

168 M. Zhou, Y. Yu, R. Chen, X. Liu, Y. Hu and Z. Ma, *et al.*, Wall shear stress and its role in atherosclerosis, *Front. Cardiovasc. Med.*, 2023, **10**, 1083547.

169 H. Cheng, W. Zhong, L. Wang, Q. Zhang, X. Ma and Y. Wang, *et al.*, Effects of shear stress on vascular endothelial functions in atherosclerosis and potential therapeutic approaches, *Biomed. Pharmacother.*, 2023, **158**, 114198.

170 K. Hattori, Y. Munehira, H. Kobayashi, T. Satoh, S. Sugiura and T. Kanamori, Microfluidic perfusion culture chip providing different strengths of shear stress for analysis of vascular endothelial function, *J. Biosci. Bioeng.*, 2014, **118**(3), 327–332.

171 M. Mohammed, P. Thurgood, C. Gilliam, N. Nguyen, E. Pirogova and K. Peter, *et al.*, Studying the Response of Aortic Endothelial Cells under Pulsatile Flow Using a Compact Microfluidic System, *Anal. Chem.*, 2019, **91**(18), 12077–12084.

172 S. Sugiura, K. Shin and T. Kanamori, Perfusion culture of endothelial cells under shear stress on microporous membrane in a pressure-driven microphysiological system, *J. Biosci. Bioeng.*, 2023, **135**(1), 79–85.

173 P. A. Galie, D. H. T. Nguyen, C. K. Choi, D. M. Cohen, P. A. Janmey and C. S. Chen, Fluid shear stress threshold regulates angiogenic sprouting, *Proc. Natl. Acad. Sci. U. S. A.*, 2014, **111**(22), 7968–7973.

174 U. M. Sonmez, Y. W. Cheng, S. C. Watkins, B. L. Roman and L. A. Davidson, Endothelial cell polarization and orientation to flow in a novel microfluidic multimodal shear stress generator, *Lab Chip*, 2020, **20**(23), 4373–4390.

175 P. Zhao, X. Liu, X. Zhang, L. Wang, H. Su and L. Wang, *et al.*, Flow shear stress controls the initiation of neovascularization via heparan sulfate proteoglycans within a biomimetic microfluidic model, *Lab Chip*, 2021, **21**(2), 421–434.

176 J. W. Wragg, S. Durant, H. M. McGettrick, K. M. Sample, S. Egginton and R. Bicknell, Shear stress regulated gene expression and angiogenesis in vascular endothelium, *Microcirculation*, 2014, **21**(4), 290–300.

177 N. Kaneko, S. Satta, Y. Komuro, S. D. Muthukrishnan, V. Kakarla and L. Guo, *et al.*, Flow-mediated Susceptibility and Molecular Response of Cerebral Endothelia to Sars-CoV-2 Infection, *Stroke*, 2020, **52**(1), 260.

178 V. A. Pozdin, P. D. Erb, M. Downey, K. R. Rivera and M. Daniele, Monitoring of random microvessel network formation by in-line sensing of flow rates: A numerical and in vitro investigation, *Sens. Actuators, A*, 2021, **331**, 112970.

179 Z. Chen, J. Zilberberg and W. Lee, Pumpless microfluidic device with open top cell culture under oscillatory shear stress, *Biomed. Microdevices*, 2020, **22**(3), 58.

180 M. N. S. de Graaf, A. Vivas, D. G. Kasi, F. E. van den Hil, A. van den Berg and A. D. van der Meer, *et al.*, Multiplexed fluidic circuit board for controlled perfusion of 3D blood vessels-on-a-chip, *Lab Chip*, 2022, **23**(1), 168–181.

181 Y. Abe, M. Watanabe, S. Chung, R. D. Kamm, K. Tanishita and R. Sudo, Balance of interstitial flow magnitude and vascular endothelial growth factor concentration modulates three-dimensional microvascular network formation, *APL Bioeng.*, 2019, **3**(3), 036102.

182 J. Kim, H. Park, H. Kim, Y. Kim, H. J. Oh and S. Chung, Microfluidic one-directional interstitial flow generation from cancer to cancer associated fibroblast, *Acta Biomater.*, 2022, **144**, 258–265.

183 V. S. Shirure, A. Lezia, A. Tao, L. F. Alonzo and S. C. George, Low levels of physiological interstitial flow eliminate morphogen gradients and guide angiogenesis, *Angiogenesis*, 2017, **20**(4), 493–504.

184 A. Figarol, M. Piantino, T. Furihata, T. Satoh, S. Sugiura and T. Kanamori, *et al.*, Interstitial flow regulates in vitro three-dimensional self-organized brain micro-vessels, *Biochem. Biophys. Res. Commun.*, 2020, **533**(3), 600–606.

185 S. Zhang, Z. Wan, G. Pavlou, A. X. Zhong, L. Xu and R. D. Kamm, Interstitial Flow Promotes the Formation of Functional Microvascular Networks In Vitro through Upregulation of Matrix Metalloproteinase-2, *Adv. Funct. Mater.*, 2022, **32**(43), 2206767.

186 G. S. Offeddu, L. Possenti, J. T. Loessberg-Zahl, P. Zunino, J. Roberts and X. Han, *et al.*, Application of Transmural Flow Across In Vitro Microvasculature Enables Direct Sampling of Interstitial Therapeutic Molecule Distribution, *Small*, 2019, **15**(46), 1902393.

187 X. Wang, D. T. T. Phan, A. Sobrino, S. C. George, C. C. W. Hughes and A. P. Lee, Engineering anastomosis between living capillary networks and endothelial cell-lined microfluidic channels, *Lab Chip*, 2016, **16**(2), 282–290.

188 S. Yuge, K. Nishiyama, Y. Arima, Y. Hanada, E. Oguri-Nakamura and S. Hanada, *et al.*, Mechanical loading of intraluminal pressure mediates wound angiogenesis by regulating the TOCA family of F-BAR proteins, *Nat. Commun.*, 2022, **13**(1), 2594.

189 J. Cacheux, A. Bancaud, D. Alcaide, J. I. Suehiro, Y. Akimoto and H. Sakurai, *et al.*, Endothelial tissue remodeling induced by intraluminal pressure enhances paracellular solute transport, *iScience*, 2023, **26**(7), 107141.

190 M. Abudupataer, S. Zhu, S. Yan, K. Xu, J. Zhang and S. Luo, *et al.*, Aorta smooth muscle-on-a-chip reveals impaired mitochondrial dynamics as a therapeutic target for aortic aneurysm in bicuspid aortic valve disease, *eLife*, 2021, **10**, e69310.

191 C. L. Thompson, T. Hopkins, C. Bevan, H. R. C. Screen, K. T. Wright and M. M. Knight, Human vascularised synovium-on-a-chip: a mechanically stimulated, microfluidic model to investigate synovial inflammation and monocyte recruitment, *Biomed. Mater.*, 2023, **18**(6), 065013.

192 L. Claesson-Welsh, E. Dejana and D. M. McDonald, Permeability of the Endothelial Barrier: Identifying and Reconciling Controversies, *Trends Mol. Med.*, 2021, **27**(4), 314–331.

193 S. Ono, G. Egawa and K. Kabashima, Regulation of blood vascular permeability in the skin, *Inflammation Regener.*, 2017, **37**(1), 11.

194 J. F. Wong and C. A. Simmons, Microfluidic assay for the on-chip electrochemical measurement of cell monolayer permeability, *Lab Chip*, 2019, **19**(6), 1060–1070.

195 M. T. Rogers, A. L. Gard, R. Gaibler, T. J. Mulhern, R. Strelnikov and H. Azizgolshani, *et al.*, A high-throughput microfluidic bilayer co-culture platform to study endothelial-pericyte interactions, *Sci. Rep.*, 2021, **11**(1), 12225.

196 Y. Qiu, B. Ahn, Y. Sakurai, C. Hansen, R. Tran and P. N. Mimche, *et al.*, Microvasculature-on-a-chip for the long-term study of endothelial barrier dysfunction and microvascular obstruction in disease, *Nat. Biomed. Eng.*, 2018, **2**, 453–463.

197 C. Hajal, G. S. Offeddu, Y. Shin, S. Zhang, O. Morozova and D. Hickman, *et al.*, Engineered human blood–brain barrier microfluidic model for vascular permeability analyses, *Nat. Protoc.*, 2022, **17**(1), 95–128.

198 C. G. M. van Dijk, M. M. Brandt, N. Poulis, J. Anten, M. van der Moolen and L. Kramer, *et al.*, A new microfluidic model that allows monitoring of complex vascular structures and cell interactions in a 3D biological matrix, *Lab Chip*, 2020, **20**(10), 1827–1844.

199 M. A. Holzreuter and L. I. Segerink, Innovative electrode and chip designs for transendothelial electrical resistance measurements in organs-on-chips, *Lab Chip*, 2024, **24**(5), 1121–1134.

200 H. Ehlers, A. Nicolas, F. Schavemaker, J. P. M. Heijmans, M. Bulst and S. J. Trietsch, *et al.*, Vascular inflammation on a chip: A scalable platform for trans-endothelial electrical resistance and immune cell migration, *Front. Immunol.*, 2023, **14**, 1118624.

201 S. Palma-Florez, A. López-Canosa, F. Morales-Zavala, O. Castaño, M. J. Kogan and J. Samitier, *et al.*, BBB-on-a-chip with integrated micro-TEER for permeability evaluation of multi-functionalized gold nanorods against Alzheimer's disease, *J. Nanobiotechnol.*, 2023, **21**(1), 115.

202 E. Akbari, G. B. Spychalski, K. K. Rangharajan, S. Prakash and J. W. Song, Flow dynamics control endothelial permeability in a microfluidic vessel bifurcation model, *Lab Chip*, 2018, **18**(7), 1084–1093.

203 G. S. Offeddu, K. Haase, M. R. Gillrie, R. Li, O. Morozova and D. Hickman, *et al.*, An on-chip model of protein paracellular and transcellular permeability in the microcirculation, *Biomaterials*, 2019, **212**, 115–125.

204 T. S. Khire, A. T. Salminen, H. Swamy, K. S. Lucas, M. C. McCloskey and R. E. Ajalik, *et al.*, Microvascular Mimetics for the Study of Leukocyte–Endothelial Interactions, *Cell. Mol. Bioeng.*, 2020, **13**(2), 125.

205 M. Shaji, A. Tamada, K. Fujimoto, K. Muguruma, S. L. Karsten and R. Yokokawa, Deciphering potential vascularization factors of on-chip co-cultured hiPSC-derived cerebral organoids, *Lab Chip*, 2024, **24**(4), 680–696.

206 S. L. Faley, N. A. Boghdeh, D. K. Schaffer, E. C. Spivey, F. Alem and A. Narayanan, *et al.*, Gravity-perfused airway-on-a-chip optimized for quantitative BSL-3 studies of SARS-CoV-2 infection: barrier permeability, cytokine production, immunohistochemistry, and viral load assays, *Lab Chip*, 2024, **24**(6), 1794–1807.

207 Y. B. Arik, W. Buijsman, J. Loessberg-Zahl, C. Cuartas-Vélez, C. Veenstra and S. Logtenberg, *et al.*, Microfluidic organ-on-a-chip model of the outer blood-retinal barrier with clinically relevant read-outs for tissue permeability and vascular structure, *Lab Chip*, 2021, **21**(2), 272–283.

208 M. Campisi, Y. Shin, T. Osaki, C. Hajal, V. Chiono and R. D. Kamm, 3D self-organized microvascular model of the human blood-brain barrier with endothelial cells, pericytes and astrocytes, *Biomaterials*, 2018, **180**, 117–129.

209 L. Ewart, A. Apostolou, S. A. Briggs, C. V. Carman, J. T. Chaff and A. R. Heng, *et al.*, Performance assessment and economic analysis of a human Liver-Chip for predictive toxicology, *Commun. Med.*, 2022, **2**(1), 1–16.

210 A. Petrosyan, P. Cravedi, V. Villani, A. Angeletti, J. Manrique and A. Renieri, *et al.*, A glomerulus-on-a-chip to recapitulate the human glomerular filtration barrier, *Nat. Commun.*, 2019, **10**(1), 3656.

211 Y. Huangfu, J. Wang, J. Feng and Z. L. Zhang, Distal renal tubular system-on-a-chip for studying the pathogenesis of influenza A virus-induced kidney injury, *Lab Chip*, 2023, **23**(19), 4255–4264.

212 S. Lee, M. Chung, S. R. Lee and N. L. Jeon, 3D brain angiogenesis model to reconstitute functional human blood-brain barrier in vitro, *Biotechnol. Bioeng.*, 2020, **117**(3), 748–762.

213 M. A. Lancaster and J. A. Knoblich, Organogenesis in a dish: Modeling development and disease using organoid technologies, *Science*, 2014, **345**(6194), 1247125.

214 J. Kim, B. K. Koo and J. A. Knoblich, Human organoids: model systems for human biology and medicine, *Nat. Rev. Mol. Cell Biol.*, 2020, **21**(10), 571–584.

215 J. J. Vandana, C. Manrique, L. A. Lacko and S. Chen, Human pluripotent-stem-cell-derived organoids for drug discovery and evaluation, *Cell Stem Cell*, 2023, **30**(5), 571.

216 X. Zhao, Z. Xu, L. Xiao, T. Shi, H. Xiao and Y. Wang, *et al.*, Review on the Vascularization of Organoids and Organoids-on-a-Chip, *Front. Bioeng. Biotechnol.*, 2021, **9**, 637048.

217 P. N. Nwokoye and O. J. Abilez, Bioengineering methods for vascularizing organoids, *Cells Rep. Methods*, 2024, **4**(6), 100779.

218 M. T. Pham, K. M. Pollock, M. D. Rose, W. A. Cary, H. R. Stewart and P. Zhou, *et al.*, Generation of human vascularized brain organoids, *NeuroReport*, 2018, **29**(7), 588–593.

219 T. Takebe, K. Sekine, M. Enomura, H. Koike, M. Kimura and T. Ogaeri, *et al.*, Vascularized and functional human liver from an iPSC-derived organ bud transplant, *Nature*, 2013, **499**(7459), 481–484.

220 Y. Jin, J. Kim, J. S. Lee, S. Min, S. Kim and D. Ahn, *et al.*, Vascularized Liver Organoids Generated Using Induced Hepatic Tissue and Dynamic Liver-Specific Microenvironment as a Drug Testing Platform, *Adv. Funct. Mater.*, 2018, **28**(37), 1801954.

221 T. Russell, Q. Dirar, Y. Li, C. Chiang, D. T. Laskowitz and Y. Yun, Cortical spheroid on perfusible microvascular network in a microfluidic device, *PLoS One*, 2023, **18**(10), e0288025.

222 E. Wang, M. J. Andrade and Q. Smith, Vascularized liver-on-a-chip model to investigate nicotine-induced dysfunction, *Biomicrofluidics*, 2023, **17**(6), 064108.

223 A. Shakeri, Y. Wang, Y. Zhao, S. Landau, K. Perera and J. Lee, *et al.*, Engineering Organ-on-a-Chip Systems for Vascular Diseases, *Arterioscler., Thromb., Vasc. Biol.*, 2023, **43**(12), 2241–2255.

224 A. Jain, A. Graveline, A. Waterhouse, A. Vernet, R. Flaumenhaft and D. E. Ingber, A shear gradient-activated microfluidic device for automated monitoring of whole blood haemostasis and platelet function, *Nat. Commun.*, 2016, **7**(1), 10176.

225 A. Jain, R. Barrile, A. D. van der Meer, A. Mammoto, T. Mammoto and K. De Ceunynck, *et al.*, Primary Human Lung Alveolus-on-a-chip Model of Intravascular Thrombosis for Assessment of Therapeutics, *Clin. Pharmacol. Ther.*, 2018, **103**(2), 332–340.

226 R. Barrile, A. D. van der Meer, H. Park, J. P. Fraser, D. Simic and F. Teng, *et al.*, Organ-on-Chip Recapitulates Thrombosis Induced by an anti-CD154 Monoclonal Antibody: Translational Potential of Advanced Microengineered Systems, *Clin. Pharmacol. Ther.*, 2018, **104**(6), 1240–1248.

227 T. Mathur, K. A. Singh, N. K. R. Pandian, S. H. Tsai, T. W. Hein and A. K. Gaharwar, *et al.*, Organ-on-chips made of blood: endothelial progenitor cells from blood reconstitute vascular thromboinflammation in vessel-chips, *Lab Chip*, 2019, **19**(15), 2500–2511.

228 L. Chen, Y. Zheng, Y. Liu, P. Tian, L. Yu and L. Bai, *et al.*, Microfluidic-based in vitro thrombosis model for studying microplastics toxicity, *Lab Chip*, 2022, **22**(7), 1344–1353.

229 Y. S. Zhang, F. Davoudi, P. Walch, A. Manbachi, X. Luo and V. Dell'Erba, *et al.*, Bioprinted thrombosis-on-a-chip, *Lab Chip*, 2016, **16**(21), 4097–4105.

230 P. F. Costa, H. J. Albers, J. E. A. Linssen, H. H. T. Middelkamp, L. van der Hout and R. Passier, *et al.*, Mimicking arterial thrombosis in a 3D-printed microfluidic in vitro vascular model based on computed tomography angiography data, *Lab Chip*, 2017, **17**(16), 2785–2792.

231 A. M. Iqbal and S. F. Jamal, Essential Hypertension, in *StatPearls [Internet]*, StatPearls Publishing, Treasure Island (FL), 2025, [cited 2025 Apr 1], Available from: <http://www.ncbi.nlm.nih.gov/books/NBK539859/>.

232 P. Martinez-Quinones, C. G. McCarthy, S. W. Watts, N. S. Klee, A. Komic and F. B. Calmasini, *et al.*, Hypertension Induced Morphological and Physiological Changes in Cells of the Arterial Wall, *Am. J. Hypertens.*, 2018, **31**(10), 1067–1078.

233 S. Oparil, M. C. Acelajado, G. L. Bakris, D. R. Berlowitz, R. Cífková and A. F. Dominiczak, *et al.*, Hypertension, *Nat. Rev. Dis. Primers*, 2018, **4**, 18014.

234 M. Humbert, G. Kovacs, M. M. Hoeper, R. Badagliacca, R. M. F. Berger and M. Brida, *et al.*, 2022 ESC/ERS Guidelines for the diagnosis and treatment of pulmonary hypertension, *Eur. Heart J.*, 2022, **43**(38), 3618–3731.

235 T. A. Al-Hilal, A. Keshavarz, H. Kadry, B. Lahooti, A. Al-Obaida and Z. Ding, *et al.*, Pulmonary-arterial-hypertension (PAH)-on-a-chip: fabrication, validation and application, *Lab Chip*, 2020, **20**(18), 3334–3345.

236 K. Soon, M. Li, R. Wu, A. Zhou, N. Khosraviani and W. D. Turner, *et al.*, A human model of arteriovenous malformation (AVM)-on-a-chip reproduces key disease hallmarks and enables drug testing in perfused human vessel networks, *Biomaterials*, 2022, **288**, 121729.

237 R. Maringanti, C. G. M. van Dijk, E. M. Meijer, M. M. Brandt, M. Li and V. P. C. Tiggeloven, *et al.*, Atherosclerosis on a Chip: A 3-Dimensional Microfluidic Model of Early Arterial Events in Human Plaques, *Arterioscler., Thromb., Vasc. Biol.*, 2024, **44**(12), 2453–2472.

238 J. Li, H. Bai, Z. Wang, B. Xu, K. N. Peters Olson and C. Liu, *et al.*, Advancements in organs-on-chips technology for viral disease and anti-viral research, *Organs-on-a-Chip*, 2023, **5**, 100030.

239 H. K. Siddiqi, P. Libby and P. M. Ridker, COVID-19 – A vascular disease, *Trends Cardiovasc. Med.*, 2021, **31**(1), 1–5.

240 P. Wang, L. Jin, M. Zhang, Y. Wu, Z. Duan and Y. Guo, *et al.*, Blood-brain barrier injury and neuroinflammation induced by SARS-CoV-2 in a lung-brain microphysiological system, *Nat. Biomed. Eng.*, 2024, **8**(8), 1053–1068.

241 R. X. Z. Lu, N. Rafatian, Y. Zhao, K. T. Wagner, E. L. Beroncal and B. Li, *et al.*, Heart-on-a-chip model of immune-induced cardiac dysfunction reveals the role of free mitochondrial DNA and therapeutic effects of endothelial exosomes, *bioRxiv*, 2023, preprint, DOI: [10.1101/2023.08.09.552495](https://doi.org/10.1101/2023.08.09.552495).

242 H. Lee, W. Park, H. Ryu and N. L. Jeon, A microfluidic platform for quantitative analysis of cancer angiogenesis and extravasation, *Biomicrofluidics*, 2014, **8**(5), 054102.

243 J. A. Nagy, S. H. Chang, A. M. Dvorak and H. F. Dvorak, Why are tumour blood vessels abnormal and why is it important to know?, *Br. J. Cancer*, 2009, **100**(6), 865.

244 S. M. Giannitelli, V. Peluzzi, S. Raniolo, G. Roscilli, M. Trombetta and P. Mozetic, *et al.*, On-chip recapitulation of the tumor microenvironment: A decade of progress, *Biomaterials*, 2024, **306**, 122482.

245 M. Tanaka, S. Chuaychob, M. Homme, Y. Yamazaki, R. Lyu and K. Yamashita, *et al.*, ASPSCR1::TFE3 orchestrates the angiogenic program of alveolar soft part sarcoma, *Nat. Commun.*, 2023, **14**(1), 1957.

246 S. Chuaychob, R. Lyu, M. Tanaka, A. Haginiwa, A. Kitada and T. Nakamura, *et al.*, Mimicking angiogenic microenvironment of alveolar soft-part sarcoma in a microfluidic coculture vasculature chip, *Proc. Natl. Acad. Sci. U. S. A.*, 2024, **121**(13), e2312472121.

247 J. P. Straehla, C. Hajal, H. C. Safford, G. S. Offeddu, N. Boehnke and T. G. Dacoba, *et al.*, A predictive microfluidic model of human glioblastoma to assess trafficking of blood-brain barrier-penetrant nanoparticles, *Proc. Natl. Acad. Sci. U. S. A.*, 2022, **119**(23), e2118697119.

248 K. Haase, G. S. Offeddu, M. R. Gillrie and R. D. Kamm, Endothelial Regulation of Drug Transport in a 3D Vascularized Tumor Model, *Adv. Funct. Mater.*, 2020, **30**(48), 2002444.

249 S. P. H. Chiang, R. M. Cabrera and J. E. Segall, Tumor cell extravasation, *Am. J. Physiol.*, 2016, **311**(1), C1.

250 I. K. Zervantonakis, S. K. Hughes-Alford, J. L. Charest, J. S. Condeelis, F. B. Gertler and R. D. Kamm, Three-dimensional microfluidic model for tumor cell extravasation and endothelial barrier function, *Proc. Natl. Acad. Sci. U. S. A.*, 2012, **109**(34), 13515.

251 Z. Xu, E. Li, Z. Guo, R. Yu, H. Hao and Y. Xu, *et al.*, Design and Construction of a Multi-Organ Microfluidic Chip Mimicking the in vivo Microenvironment of Lung Cancer Metastasis, *ACS Appl. Mater. Interfaces*, 2016, **8**(39), 25840–25847.

252 W. Liu, J. Song, X. Du, Y. Zhou, Y. Li and R. Li, *et al.*, AKR1B10 (Aldo-keto reductase family 1 B10) promotes brain metastasis of lung cancer cells in a multi-organ microfluidic chip model, *Acta Biomater.*, 2019, **91**, 195–208.

253 J. S. Jeon, S. Bersini, M. Gilardi, G. Dubini, J. L. Charest and M. Moretti, *et al.*, Human 3D vascularized organotypic microfluidic assays to study breast cancer cell extravasation, *Proc. Natl. Acad. Sci. U. S. A.*, 2015, **112**(1), 214–219.

254 M. B. Chen, J. A. Whisler, J. S. Jeon and R. D. Kamm, Mechanisms of tumor cell extravasation in an in vitro microvascular network platform, *Integr. Biol.*, 2013, **5**(10), 1262–1271.

255 J. Song, A. Miermont, C. T. Lim and R. D. Kamm, A 3D microvascular network model to study the impact of hypoxia on the extravasation potential of breast cell lines, *Sci. Rep.*, 2018, **8**(1), 17949.

256 F. L. Miles, F. L. Pruitt, K. L. van Golen and C. R. Cooper, Stepping out of the flow: capillary extravasation in cancer metastasis, *Clin. Exp. Metastasis*, 2008, **25**(4), 305–324.

257 A. F. Chambers, A. C. Groom and I. C. MacDonald, Dissemination and growth of cancer cells in metastatic sites, *Nat. Rev. Cancer*, 2002, **2**(8), 563–572.

258 I. J. Fidler, The pathogenesis of cancer metastasis: the “seed and soil” hypothesis revisited, *Nat. Rev. Cancer*, 2003, **3**(6), 453–458.

259 Y. Sakurai, E. T. Hardy and W. A. Lam, Hemostasis-on-a-chip/incorporating the endothelium in microfluidic models of bleeding, *Platelets*, 2023, **34**(1), 2185453.

260 Y. Sakurai, E. T. Hardy, B. Ahn, R. Tran, M. E. Fay and J. C. Ciciliano, *et al.*, A microengineered vascularized bleeding model that integrates the principal components of hemostasis, *Nat. Commun.*, 2018, **9**(1), 509.

261 I. Poventud-Fuentes, K. W. Kwon, J. Seo, M. Tomaiuolo, T. J. Stalker and L. F. Brass, *et al.*, A Human Vascular Injury-on-a-Chip Model of Hemostasis, *Small*, 2021, **17**(15), 2004889.

262 S. K. Yadav, S. Park, Y. M. Lee, S. Hurh, D. Kim and S. Min, *et al.*, Application of microphysiologic system to assess neutrophil extracellular trap in xenotransplantation, *J. Immunol. Methods*, 2023, **521**, 113537.

263 S. Rajasekar, D. S. Y. Lin, L. Abdul, A. Liu, A. Sotra and F. Zhang, *et al.*, IFlowPlate—A Customized 384-Well Plate for the Culture of Perfusionable Vascularized Colon Organoids, *Adv. Mater.*, 2020, **32**(46), 2002974.

264 D. C. Wimalachandra, Y. Li, J. Liu, S. Shikha, J. Zhang and Y. C. Lim, *et al.*, Microfluidic-Based Immunomodulation of Immune Cells Using Upconversion Nanoparticles in Simulated Blood Vessel-Tumor System, *ACS Appl. Mater. Interfaces*, 2019, **11**(41), 37513–37523.

265 J. M. Ayuso, R. Truttschel, M. M. Gong, M. Humayun, M. Virumbrales-Munoz and R. Vitek, *et al.*, Evaluating natural killer cell cytotoxicity against solid tumors using a microfluidic model, *Onco Targets Ther*, 2018, **8**(3), 1553477.

266 M. Humayun, J. M. Ayuso, K. Y. Park, B. M. Di Genova, M. C. Skala and S. C. Kerr, *et al.*, Innate immune cell response to host-parasite interaction in a human intestinal tissue microphysiological system, *Sci. Adv.*, 2022, **8**(18), eabm8012.

267 S. Kim, M. Chung and N. L. Jeon, Three-dimensional biomimetic model to reconstitute sprouting lymphangiogenesis in vitro, *Biomaterials*, 2016, **78**, 115–128.

268 P. Fathi, G. Holland, D. Pan and M. B. Esch, Lymphatic Vessel on a Chip with Capability for Exposure to Cyclic Fluidic Flow, *ACS Appl. Bio Mater.*, 2020, **3**(10), 6697–6707.

269 A. R. Henderson, H. Choi and E. Lee, Blood and Lymphatic Vasculatures On-Chip Platforms and Their Applications for Organ-Specific In Vitro Modeling, *Micromachines*, 2020, **11**(2), 147.

270 A. Crnic, S. Rohringer, T. Tyschuk and W. Holnthoner, Engineering blood and lymphatic microvascular networks, *Atherosclerosis*, 2024, **393**, 117458.

271 T. I. Maulana, C. Teufel, M. Cipriano, J. Roosz, L. Lazarevski and F. E. Van Den Hil, *et al.*, Breast cancer-on-chip for patient-specific efficacy and safety testing of CAR-T cells, *Cell Stem Cell*, 2024, **31**(7), 989–1002.e9.

272 Z. Wan, M. A. Floryan, M. F. Coughlin, S. Zhang, A. X. Zhong and S. E. Shelton, *et al.*, New Strategy for Promoting Vascularization in Tumor Spheroids in a Microfluidic Assay, *Adv. Healthcare Mater.*, 2023, **12**(14), 2201784.

273 J. D. Joy, B. Malacrida, F. Laforêts, P. Kotantaki, E. Maniati and R. Manchanda, *et al.*, Human 3D Ovarian Cancer Models Reveal Malignant Cell-Intrinsic and -Extrinsic Factors That Influence CAR T-cell Activity, *Cancer Res.*, 2024, **84**(15), 2432–2449.

274 J. Vasudevan, R. Vijayakumar, J. A. Reales-Calderon, M. S. Y. Lam, J. R. Ow and J. Aw, *et al.*, In vitro integration of a functional vasculature to model endothelial regulation of chemotherapy and T-cell immunotherapy in liver cancer, *Biomaterials*, 2025, **320**, 123175.

275 J. J. Han, FDA Modernization Act 2.0 allows for alternatives to animal testing, *Artif. Organs*, 2023, **47**(3), 449–450.

276 D. Kim, K. S. Hwang, E. U. Seo, S. Seo, B. C. Lee and N. Choi, *et al.*, Vascularized Lung Cancer Model for Evaluating the Promoted Transport of Anticancer Drugs and Immune Cells in an Engineered Tumor Microenvironment, *Adv. Healthcare Mater.*, 2022, **11**(12), 2102581.

277 P. Yavvari, A. Laporte, L. Elomaa, F. Schraufstetter, I. Pacharzina and A. D. Daberkow, *et al.*, 3D-Cultured Vascular-Like Networks Enable Validation of Vascular Disruption Properties of Drugs In Vitro, *Front. Bioeng. Biotechnol.*, 2022, **10**, 888492.

278 H. Wang, W. Zhu, C. Xu, W. Su and Z. Li, Engineering organoids-on-chips for drug testing and evaluation, *Metabolism*, 2024, **162**, 156065.

279 D. T. T. Phan, X. Wang, B. M. Craver, A. Sobrino, D. Zhao and J. C. Chen, *et al.*, A vascularized and perfused organ-on-a-chip platform for large-scale drug screening applications, *Lab Chip*, 2017, **17**(3), 511–520.

280 J. Yu, S. Lee, J. Song, S. R. Lee, S. Kim and H. Choi, *et al.*, Perfusionable micro-vascularized 3D tissue array for high-throughput vascular phenotypic screening, *Nano Convergence*, 2022, **9**(1), 16.

281 C. Soragni, K. Queiroz, C. P. Ng, A. Stok, T. Olivier and D. Tzagkaraki, *et al.*, Phenotypic screening in Organ-on-a-Chip systems: a 1537 kinase inhibitor library screen on a 3D angiogenesis assay, *Angiogenesis*, 2024, **27**(1), 37–49.

282 J. C. Mejias, M. R. Nelson, O. Liseth and K. Roy, A 96-well format microvascularized human lung-on-a-chip platform for microphysiological modeling of fibrotic diseases, *Lab Chip*, 2020, **20**(19), 3601–3611.

283 S. Zhu, M. Abudupataer, S. Yan, C. Wang, L. Wang and K. Zhu, Construction of a high-throughput aorta smooth muscle-on-a-chip for thoracic aortic aneurysm drug screening, *Biosens. Bioelectron.*, 2022, **218**, 114747.

284 H. T. Tzeng and Y. J. Huang, Tumor Vasculature as an Emerging Pharmacological Target to Promote Anti-Tumor Immunity, *Int. J. Mol. Sci.*, 2023, **24**(5), 4422.

285 Y. A. Chen, Y. C. Tsai, Y. D. Chen, D. Z. Liu, T. H. Young and L. K. Tsai, Intraventricular Medium B Treatment Benefits an Ischemic Stroke Rodent Model via Enhancement of Neurogenesis and Anti-apoptosis, *Sci. Rep.*, 2020, **10**(1), 6596.